

JPRS 78677

5 August 1981

China Report

SCIENCE AND TECHNOLOGY

No. 116



FOREIGN BROADCAST INFORMATION SERVICE

NOTE

JPRS publications contain information primarily from foreign newspapers, periodicals and books, but also from news agency transmissions and broadcasts. Materials from foreign-language sources are translated; those from English-language sources are transcribed or reprinted, with the original phrasing and other characteristics retained.

Headlines, editorial reports, and material enclosed in brackets [] are supplied by JPRS. Processing indicators such as [Text] or [Excerpt] in the first line of each item, or following the last line of a brief, indicate how the original information was processed. Where no processing indicator is given, the information was summarized or extracted.

Unfamiliar names rendered phonetically or transliterated are enclosed in parentheses. Words or names preceded by a question mark and enclosed in parentheses were not clear in the original but have been supplied as appropriate in context. Other unattributed parenthetical notes within the body of an item originate with the source. Times within items are as given by source.

The contents of this publication in no way represent the policies, views or attitudes of the U.S. Government.

PROCUREMENT OF PUBLICATIONS

JPRS publications may be ordered from the National Technical Information Service, Springfield, Virginia 22161. In ordering, it is recommended that the JPRS number, title, date and author, if applicable, of publication be cited.

Current JPRS publications are announced in Government Reports Announcements issued semi-monthly by the National Technical Information Service, and are listed in the Monthly Catalog of U.S. Government Publications issued by the Superintendent of Documents, U.S. Government Printing Office, Washington, D.C. 20402.

Indexes to this report (by keyword, author, personal names, title and series) are available from Bell & Howell, Old Mansfield Road, Wooster, Ohio 44691.

Correspondence pertaining to matters other than procurement may be addressed to Joint Publications Research Service, 1000 North Glebe Road, Arlington, Virginia 22201.

5 August 1981

CHINA REPORT
SCIENCE AND TECHNOLOGY

No. 116

CONTENTS

PHYSICAL SCIENCES

Energy of 1908 Siberian Meteorite Explosion Calculated (Hu Xinkang; SHENGXUE XUEBAO, No 3, 1981)	1
Oceanic Sound Signal Transmission Channels Studied (Chen Geng; SHENGXUE XUEBAO, No 3, 1981)	9
Sound Wave Propagation in Kaolinite Suspension Studied (Tang Yingwu; SHENGXUE XUEBAO, No 3, 1981)	23

LIFE SCIENCES

Electric Shock Therapy Used in Epilepsy Treatment (Wang Zucheng, et al; ZHONGHUA SHENJING JINGSHENKE ZAZHI, No 1, 1981)	38
Clinical Data, by Wang Zucheng, et al. Clinical Analysis, by Lu Longguang, et al.	

PHYSICAL SCIENCES

ENERGY OF 1908 SIBERIAN METEORITE EXPLOSION CALCULATED

Beijing SHENGXUE XUEBAO [ACTA ACUSTICA] in Chinese No 3, 1981 pp 142-147

[Article by Hu Xinkang [5170 9515 1660] of the Acoustics Institute of the Chinese Academy of Sciences: "Calculation of the Energy Released by the Great Meteorite Explosion From Infrasonic Data"]

[Text] This article proposes the use of infrasonic waves generated by a big explosion in the atmosphere to calculate the energy released by the explosion. We used this method to calculate the energy released by the explosion of the large meteor close to the ground in Central Siberia in the Soviet Union on 30 June 1908 to be $(2.3 \pm 1.5) \times 10^{24}$ erg, and compared this with other computed results.

I. Introduction

At 0016.2 hours on 30 June 1908 (Greenwich Mean Time), a large meteor exploded violently close to the ground in the Tunguska region of the great forest in Soviet Central Siberia. This incident shook the world at the time. Related scientific research is still being carried out today based on the information obtained at the time. In recent years, research has become more profound in the attempt to understand the nature of this incident.

At the time of explosion of the falling meteor, strong infrasonic waves were produced. These infrasonic waves were recorded by the microbarometers (Show and W.H. Dines, 1905) that had just been successfully developed and that were being used at several localities throughout the world. But because the mechanism of propagation of infrasound through the atmosphere at the time was poorly understood, the research results obtained from the data varied greatly (1-6).

This article proposes a method of calculation of the energy released by the explosion of the falling meteor based on the theory of infrasonic waveforms (7-8). The accuracy of the results is onefold, the true value may be between one-half and two times the calculated value. From the 1950's to the 1970's, many methods of estimation have been proposed but almost without exception, they can only

*This article was received on 13 June 1980

assure an accuracy of about 5 times (the true value may be between one-half and five times the calculated value) (9-16).

We have used our method to calculate the amount of energy released by the explosion of the largest falling meteor as yet known to mankind and compared it with the results obtained by various previous methods.

II. Computational Formula

According to the theory of infrasonic waveforms, the infrasonic wave pressure produced on the ground surface at a horizontal distance R from an explosion in the atmosphere is given by the following equation (7, 8):

$$P = \sum_n P_n(R, \theta, z_0, z, t) \quad (1)$$

where sound pressure P is the sum of the n simple normal waves of sound pressure, and the simple normal wave of sound pressure is given by the following equation:

$$P_n = \int D_n F(\omega) d\omega \quad (2)$$

where

$$D_n = \left[\frac{\rho_0(z)}{\rho_0(z_0)} \right]^{1/2} \left[\frac{2k}{\pi R} \right]^{1/2} \frac{Y_{kT}^{1/2} [P_0(z_0)/P_0(0)]^{1/2} L_p P_s}{[\omega^2 + (\lambda_0 Y_{kT}^{1/2} t_s)^{-2}]} \times M \quad (3)$$

The meaning of the parameters in equations (1), (2) and (3) is as follows:

R is the horizontal distance between the origin of explosion and the observation point, z_0 is the altitude of the explosion, z is the altitude of the observation point, Y_{kT} is the energy of explosion, k is the number of waves, ρ_0 is the density, M is the acoustic channel factor, θ is the azimuth of the observation point, ω is the angular frequency, λ_0 is the ratio factor ≈ 1 .

L_p , P_s , t_s are constants; their values are respectively 1 km, $1.61 \times 34.45 \times 10^2$ Pa, and $t_s = 0.48$ s.

t is the observation time.

For a large explosion in the atmosphere, the main frequency of the pressure wave received at a distant locality (for example, the magnitude of the main angular frequency of the infrasonic wave column received at a locality several thousand kilometers from the origin of the explosion equivalent to 1000 kT of TNT is below 1/100), therefore we have:

$$\omega^2 \ll (\lambda_0 Y_{kT}^{1/2} t_s)^{-2} \quad (4)$$

Substituting this into equation (1) we obtain:

$$P = R^{1/2} \cdot Y_{\text{eff}} \cdot \sum_s G_s(\omega, z_0) \quad (5)$$

where $\sum_s G_s(\omega, z_0)$ in equation (5) is of course a complicated function.

It is a function of the altitude of explosion, frequency and acoustic channel factor. Theoretical and experimental research shows that for such an explosion far below the subsonic channel altitude, the altitude of explosion has almost no effect upon the oscillating waveform or the amplitude. The subsonic channel altitude is generally about 25 kilometers above the ground. Therefore, within the range of 0 to 3 kilometers above the ground surface, we can regard this as satisfactory. Also, many people (such as Scorer, Pekeris, Harkrider and Pierce) have shown in their research that regardless of whether the model of multiple atmospheric strata, double atmospheric strata or single atmospheric strata is used, the foremost parts of the column of infrasonic waves (the first three cycles) are basically the same. This means that the acoustic channel factor (which is atmospheric structure) affects the foremost parts of the infrasonic wave column very slightly, and therefore, if we only take the various parameters of the foremost parts of the wave column, then the acoustic factor M can be approximated as a constant (11).

Obviously, under the above conditions, $\sum_s G_s(\omega, z_0)$ is only a function of angular frequency ω (or period T). According to the results of processing a large amount of experimental data (17), we have finally obtained a simple formula to calculate the energy:

$$Y = C \cdot P \cdot T \cdot R^{1/2} \quad (6)$$

where
Y--energy released by the explosion, in unit erg;
C--empirical constant, with a value of 8×10^{19} ;
P--sound pressure of the column of infrasonic waves, in unit Pa;
T--main cycle of the column of infrasonic waves, in unit s;
R--distance between the point of explosion and the point of observation, in unit Mm.

According to the large amount of practice of many years, the accuracy of the results of calculation using this method can reach within onefold.

III. Study of the Energy Released by the Big Meteoric Explosion of 1908

Figure 1 shows the center of explosion and the recording stations at the various localities in the world. The longitude and latitude of the center of explosion is E $101^{\circ} 57'$, N $60^{\circ} 54'$. The author has organized the data and information of the time which have been gathered in Table 1. The table lists 10 receiving stations; actually, the reception at the Greenwich station is a composite of six independent receiving stations. It can be seen from the actual data that the information gathered by England and by the Soviet Union itself are the most complete. Figures 2 and 3 are two typical infrasonic wave column diagrams.

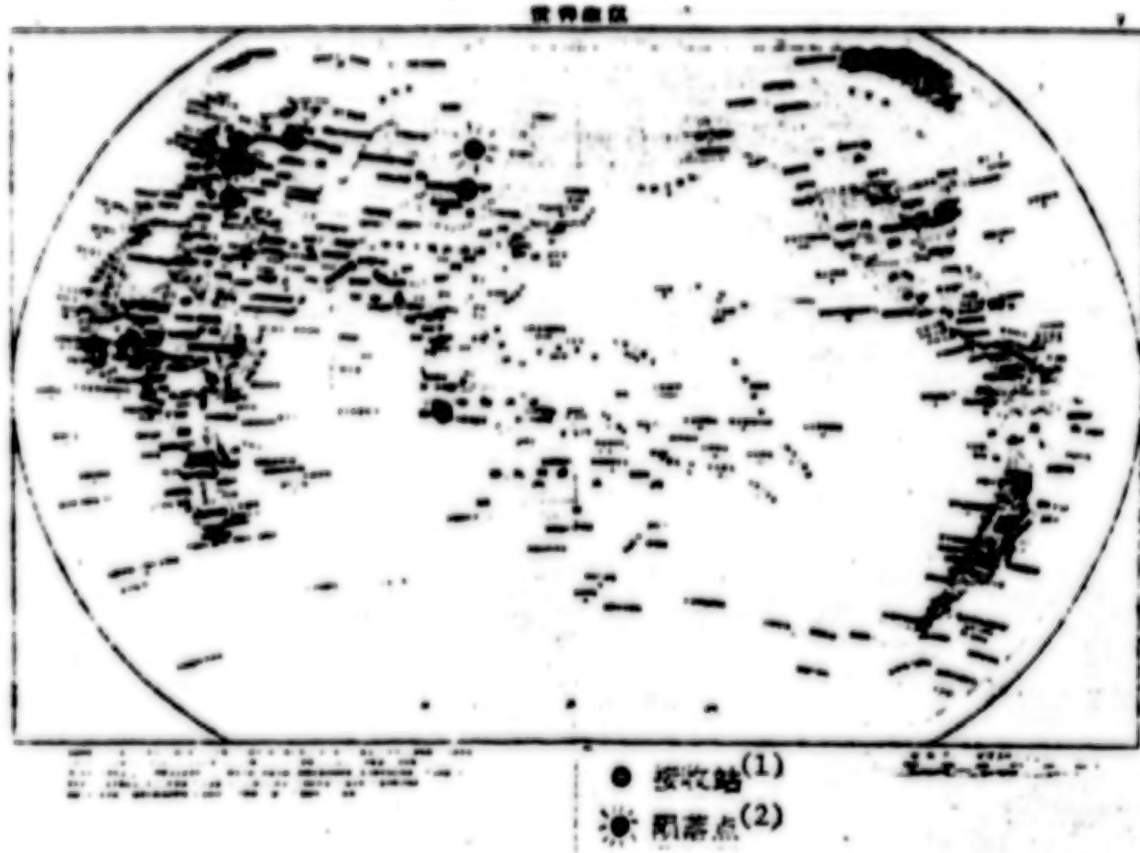
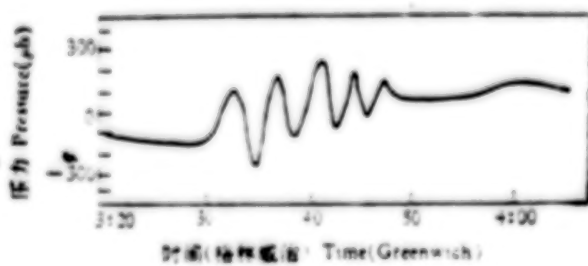


Figure 1. Schematic Map of the Great Siberian Explosion Area and the Infrasound Stations on 30 June 1908.

*The base map was taken from the world map of political regions in the world atlas published by the Map Publishing Agency in 1978.

Key: (1) Receiving station (2) Point of impact of the meteor.



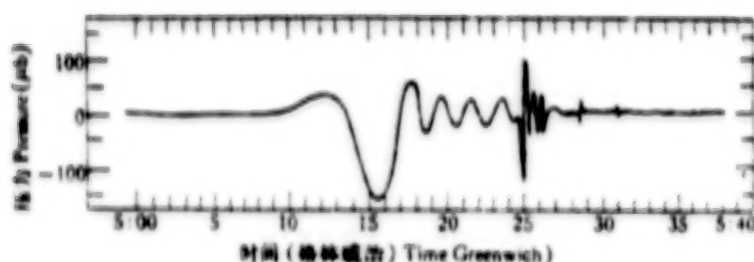


Figure 3. The Record of Infrasound Produced by the Explosion as Received at Greenwich (England).

Table 1. Detailed Data of the Infrasounds According to the Central Siberia Meteorite on 30 June 1908

(1) 站名	(2) 纬度	(3) 经度	(4) 频率点与接收站间距离 (km)	(5) 声压 (Pa)	(6) 主周期 (s)	(7) 方位角 (deg)
伊尔库茨克 Irkusk	52°16' N	104°19' E	970	120	180	170
斯普茨克 Sluszk	59°41' N	30°29' E	3740	30	257	302
哥本哈根 Copenhagen	55°40' N	12°30' E	4840	25		305
柏林 Berlin	52°32' N	13°25' E	5050	30		301
波茨坦 Potsdam	52°24' N	13°04' E	5080	76		302
斯克里柯普 Schneekoppe	50°44' N	15°43' E	5090	30		299
萨格勒布 Zagreb	45°49' N	15°59' E	5490	27		294
格林威治 Greenwich	51°29' N	0°0'	5740	20	465	309
雅加达 Batavia*	6°11' S	106°50' E	7470	13		175
华盛顿 Washington	38°54' N	77°03' W	8910	10		359

(8) Batavia 为雅加达原英文名称。

Key :

(1) Station name	(5) Sound pressure
(2) Latitude	(6) Main cycles (s)
(3) Longitude	(7) Azimuth (deg)
(4) Distance between the point of impact and receiving station (km)	(8) Batavia is the original English name of Djakarta

The simple normal waves in Figure 2 are basically superposed, while the simple normal waves in Figure 3 have basically been clearly separated. The frequency scattering characteristic can be clearly seen.

Using the data of the 10 stations of the world listed in Table 1 and formula (6), we can calculate the energy released by the explosion of this falling meteor from the data of each station. The total of the results of these 10 stations gives the average value and the standard deviation. The results are listed in Table 2. Finally, we conclude that the energy released by the explosion of this falling meteor was $(2.3 \pm 1.5) \times 10^{24}$ erg.

Table 2. Calculated Energy of the Big Siberian Meteorite Explosion

(1) 站名	(2) 能量(erg)	(3) 站名	(4) 能量(erg)
(5) 伊尔库茨克	1.7×10^{24}	(11) 施特拉布	2.4×10^{24}
(6) 斯拉夫	1.3×10^{24}	(12) 格林威治	1.8×10^{24}
(7) 哥本哈根	1.8×10^{24}	(13) 巴加达	1.3×10^{24}
(8) 柏林	2.6×10^{24}	(14) 华盛顿	1.1×10^{24}
(9) 波茨坦	6.4×10^{23}		
(10) 斯诺伊柯普	2.5×10^{24}	(15) 能量平均值*	$(2.3 \pm 1.5) \times 10^{24}$

* 是误差标准偏差。(16)

Key:

(1) Station name	(9) Potsdam
(2) Energy (erg)	(10) Schneekoppe
(3) Station name	(11) Zagreb
(4) Energy (erg)	(12) Greenwich
(5) Irkutsk	(13) Batavia
(6) Slutsk	(14) Washington
(7) Copenhagen	(15) Average value of energy*
(8) Berlin	(16) *The error is standard deviation

From 1925 to the present, many methods have already been used to study the energy released by the explosion of this falling meteor, the details of which are listed in the appendix. The estimated value of the energy is from 10^{17} to 10^{24} erg. The range reaches 7 degrees of magnitude. The estimated mass is from 13 tons to 500 tons, a range of over 5 degrees of magnitude.

We should point out one thing in our calculations: for the main cycles about 5,000 kilometers apart, we have used the values of the Greenwich station. The reason we can do this is that at such distances, further frequency scattering of each simple normal wave becomes very weak. Of course, with more complete data, this is unnecessary.

APPENDIX

The values of the energy released by the explosion of this falling meteor derived (or estimated) by the various methods used from 1925 to 1980 are as follows:

1. The method of using the audible threshold of audible sound produced a power of $> 10^{17}$ erg/s;
2. Comparison with the big explosion of the Krakatoa volcano in 1883 gave an energy of $< 10^{21}$ erg;
3. Comparison with the strong winds of 50 meters per second gave a power of $> 5 \times 10^{23}$ erg/s;

4. Comparison with earthquakes gave an energy of $\leq 10^{21}$ erg;
5. Estimates based on the height of the columns of fire and the intensity of light at the time of explosion gave a power of 2×10^{19} to 10^{24} erg/s;
6. Estimates based on the area of forests and trees destroyed by the shock waves of the explosion gave an energy of $> 4.4 \times 10^{21}$ erg;
7. Estimates based on atmospheric fluctuations in the Soviet Union gave an energy of $> 0.5 \times 10^{20}$ erg;
8. Estimates based on atmospheric fluctuations in England gave an energy of $> 3.2 \times 10^{20}$ erg;
9. Comparison with the series of atmospheric nuclear tests conducted over Novaya Zemlya in the 1960's by the Soviet Union gave an energy of about 10^{24} erg in magnitude;
10. Estimates based on the depth and the dimension of the meteor crater gave a mass of about 13 tons;
11. Estimates based on the greatest possible velocity of a meteor of the solar system entering the earth's atmosphere gave a mass of at least 30,000 tons;
12. The Ukrainian Academy of Sciences of the USSR calculated the mass of the meteor to be over 5 million tons on the basis of the distribution of isotopic microscopic granules and power of the explosion.

REFERENCES

1. Whipple, F. J. W., "The Great Siberian Meteor and the Waves, Seismic and Aerial, Which It Produced," Q. J. R. Meteor. Soc., 56(1930), 287-304.
2. Astapowitsch, I. S., "Air Waves Caused by the Fall of the Meteorite on 30th June 1908, in Central Siberia," Q. J. R. Meteor. S., 60 (1934), 493-504.
3. Jones, R. V., C. B., C. B. E., "Subacoustic Waves From Large Explosions," Nature, 193(1962), No 4812, 229-232.
4. Russell, S., "Brilliant Sky Glows, 30 June and 1 July 1908," Q. J. R. Meteor. Soc., 34(1908), 202.
5. Pekeris, C. L., "The Propagation of a Pressure Pulse in the Atmosphere," Phys. Rev., 73(1948), 145-154.
6. Gossard, E. E. and Hooke, W. H., "Waves in the Atmosphere," (Elsevier Scientific Publishing Company, New York, 1975).

7. Hirshler, D. G., "Theoretical and Observed Acoustical Waves From Explosion Sources in the Atmosphere," J. Geophys. Res., 69(1964).
8. Pierce, A. D. and Posey, J. W., "Theoretical Prediction of Acoustic-Gravity Pressure Waveform Generated by Large Explosion in the Atmosphere," AFCLR-70-0134, 30 April (1970).
9. Pierce, A. D. and Posey, J. W., "Theory of the Excitation and Propagation of Lamb S Atmospheric Edge Mode From Nuclear Explosion," G. J. R. Astr. Soc., 26(1971).
10. Letter, R., Merbst, R. F. and Watson, K. M., "Detection of Nuclear explosion," AD 604532, 2 Aug. (1961).
11. Pierce, A. D., Posey, J. W. and Ilff, F., "Variation of Nuclear Explosion Generated Acoustic Gravity Waveforms With Burst Height and With Energy Yield," J. Geophys. Res., 76(1971), 5025-5042.
12. Posey, J. W. and Pierce, A. D., "Estimation of Nuclear Explosion Energy From Microbarograph Records," Nature, 23(1971), July No 253, 232.
13. Flores, J. W. and Vega, A. J., "Some Relation Between Energy Yield of Atmospheric Nuclear Tests and Generated Infrasonic Waves," J.A.S.A., 57(1975), No 5.
14. Weston, V. H., "The Pressure Pulse Produced by a Large Explosion in the Atmosphere, Part 2," Can. J. Phys. 40(1962), 431-445.
15. Murayama, N., "Pressure Waves Produced by the Large Nuclear Explosion in 1961-1962," J. Meteo. Res. 15(1963), No 3.
16. Mackinnon, R. F., "Microbarographic Oscillations Produced by Nuclear explosion as Recorded in Great Britain and Eire," Q. J. R. Meteo. Soc. 94(1968).
17. Hu Xinkang [5170 1800 1660], Fan Yuanchun [5400 0337 2504], Qian Zhisheng [6929 1807 3932], "Method of Calculating the Energy of Strong Pulses of Sonic Sources in the Atmosphere," abstract of the papers presented at the Second National Acoustics Academic Conference, (Chinese Acoustics Society, Beijing, 1979, 5).

4706
157: 4008/367

OCEANIC SOUND SIGNAL TRANSMISSION CHANNELS STUDIED

Beijing SHENGXUE XUEBAO [ACTA ACUSTICA] in Chinese No 3, 1981 pp 152-161

[Article by Chen Geng [7115 1649] and Xu Junhun [1776 0193 5478] of the Acoustics Institute of the Chinese Academy of Sciences: "Using the Method of Correlation Between Signal Pulses To Measure the Time-Variant Characteristics of Oceanic Sound Signal Transmission Channels"]

[Text] This article presents a method of correlation between signal pulses to study the random time-variant characteristics of oceanic sound signal transmission channels. It derives the expression of the correlation function between periodic pulses transmitted through a sound signal transmission channel and gives the results of measurement of the correlation coefficients between the pulse transmitted through the sound signal transmission channel and the pulse in the reflection channel of a fixed target, and it gives a preliminary analysis of the model of the communications channel and the results of measurement.

I. Correlation Between Pulses and the Model of the Communications Channel

1. Derivation of the Correlation Function of Pulses of Time Variant Communications Channels

In recent years, a lot of research concerning underwater acoustic communications channels has pointed out (1-3) that because of the effects of scattering and refraction caused by undulations of surface waves of the ocean, unevenness and unsmoothness of the layers of the bottom of the sea and unevenness of the aquatic media of sea water, the actual oceanic sound signal transmission channel is not only multiple but it is also randomly variable in time and space. We can regard the underwater sound signal channel between the receiving point and the fixed transmission point as a linear random variable wave filter whose time-variant characteristics can be described systematically by a correlation function:

$$R_H(i\omega_1, t_1, \Delta\omega, \tau) = E[H(i\omega_1, t_1)H^*(i\omega_2, t_2)] \quad (1)$$

*This article was received on 18 December 1979.

where $H(\omega, t)$ is the transfer function of the time-variant system.

The input and output relationship (Figure 1) of the linear system can be represented by

$$Y(t) = \int_{-\infty}^t h(t - \tau, \tau) X(\tau) d\tau = \int_0^t h(\tau, \tau) X(t - \tau) d\tau \quad (2)$$

where

$$h(\tau, t) = \frac{1}{2\pi} \int_{-\infty}^{\infty} H(i\omega, t) e^{i\omega\tau} d\omega \quad (3)$$

The expression of the correlation function of the system's output $Y(t)$ is

$$\begin{aligned} R_y(t_k, t_n) &= E[Y(t_k)Y(t_n)] \\ &= E \left[\int_0^{t_k} h(u_k, t_k) h(u_n, t_n) X(t_k - u_k) X(t_n - u_n) du_k du_n \right] \end{aligned}$$

k, n represent the labels of the sample points at times t_k and t_n in the random process $Y(t)$. If X and h are statistically independent, then

$$\begin{aligned} R_y(t_k, t_n) &= \iint_0^{t_k} E[h(u_k, t_k)h(u_n, t_n)] \cdot E[X(t_k - u_k)X(t_n - u_n)] du_k du_n \\ &= \iint_0^{t_k} E[h(u_k, t_k)h(u_n, t_n)] \cdot R_x(t_k - u_k, t_n - u_n) du_k du_n \end{aligned} \quad (4)$$

where R_x is the correlation function of the input signal.

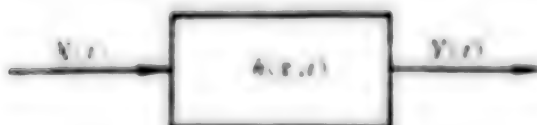


Figure 1. Schematic Diagram of a Time-Variant System

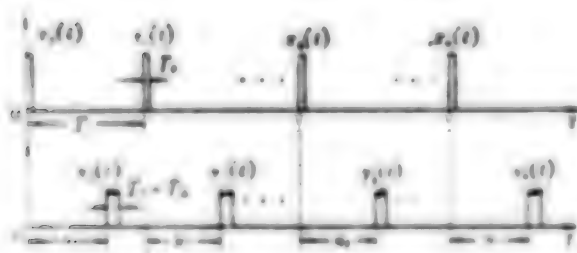


Figure 2. Schematic Illustration of the Response of the Channel System to Periodic Pulses

If a determined periodically repetitive signal $X(t + mT)$ is sent at the system's input end, we can refer to the input and output timetable to define the range

$$\begin{aligned} X_m(t) &= X(mT + t) \quad [mT, mT + T_s] \\ Y_m(t) &= Y(mT + s_m + t) \quad [mT + s_m, mT + s_m + T_s + T_h] \\ m &= 0, 1, 2, \dots, N-1, \end{aligned}$$

where T_s -- the width of the pulse of the input signal;

T_h -- time expansion caused by the communications channel.

$$Y_t(t) = Y(t_t) = \int_0^T \delta(u_t, t_t) X(t_t - u_t) du_t \quad (5)$$

$$Y_s(t) = Y(t_s) = \int_0^T \delta(u_s, t_s) X(t_s - u_s) du_s \quad (6)$$

We then delay $Y_s(t)$ which has been received first to find the correlation function between the pulses $Y_{t_k}(t)$ and $Y_{s_l}(t)$. Let

$$t_{s_l} = t_k + \tau' \quad (7)$$

In equation (7), τ' is the delay time; for convenience, the apostrophe will be omitted.

$$\begin{aligned} R_s(t_k, t_k + \tau) &= \frac{1}{T} \int_0^T Y(t_k) Y(t_k + \tau) dt_k \\ &= \frac{1}{T} \left\{ \int_0^T \int_0^T \delta(u_k, t_k) \delta(u_s, t_k + \tau) X(t_k - u_k) X(t_k + \tau - u_s) du_k du_s dt_k \right\} \end{aligned} \quad (8)$$

If the system is wide-sense stationary, and if we assume that the response function of the communications channel varies relatively slowly with t_s in the interval $(0, T)$, then we can obtain the following by approximation

$$\begin{aligned} R_s(\tau) &\approx \int_0^T \int_0^T \delta(u_k, \bar{t}) \delta(u_s, \bar{t} + \tau) \left[\frac{1}{T} \int_0^T X(t_k - u_k) X(t_k + \tau - u_s) dt_k \right] du_k du_s, \\ &= \int_0^T \int_0^T \delta(u_k, \bar{t}) \delta(u_s, \bar{t} + \tau) R_s(\tau + u_k - u_s) du_k du_s. \end{aligned} \quad (9)$$

\bar{t} represent the average value over the area of integration. We calculate the statistical average of λ , η on both sides of equation (9)

$$E[R_s(\tau)] = E \int_0^T \int_0^T \delta(u_k, \bar{t}) \delta(u_s, \bar{t} + \tau) R_s(\tau + u_k - u_s) du_k du_s.$$

and exchange the order of E and the integration symbol and take into consideration the fact that X is the determined signal

$$R_s(\tau) = \iint_0^{\infty} E(s(u_k, i)h(u_s, i + \tau)) R_s(\tau + u_k - u_s) du_k du_s \quad (10)$$

It can be seen that when there is a periodic determined signal at the input end of the system, the correlation function $R_y(\tau)$ of $Y(t)$ at the output end of the system is the special case of equation (4).

Substituting equation (3) into equation (10), we have

$$R_s(\tau) = \frac{1}{4\pi^2} \iint_{-\infty}^{\infty} \iint_0^{\infty} E(H(i\omega_k, i)H^*(i\omega_s, i + \tau)) R_s(\tau + u_k - u_s) \\ \cdot e^{i\omega_k u_k - i\omega_s u_s} du_k du_s d\omega_k d\omega_s$$

Because when $t < 0$, $h(u_k, t_p) = h(u_k, t_b) = 0$, and the zero limit of the integral can be changed to $-\infty$, then substituting equation (1) into the above equation

$$= \frac{1}{4\pi^2} \iint_{-\infty}^{\infty} \iint_0^{\infty} R_H(\omega_k, \Delta\omega, \tau) \cdot R_s(\tau + u_k - u_s) e^{i\omega_k u_k - i\omega_s u_s} \\ \cdot du_k du_s d\omega_k d\omega_s \quad (11)$$

where $\Delta\omega = \omega_k - \omega_s$.

Also because of integration

$$\iint_0^{\infty} R_s(\tau + u_k - u_s) e^{i\omega_k u_k - i\omega_s u_s} du_k du_s \\ = \iint_0^{\infty} R_s(\tau + s) e^{is\omega_k} \cdot e^{i(\omega_k - \omega_s)s} ds du_s \\ = X(\omega_k) e^{-is\omega_k} \delta(\omega_k - \omega_s) \quad (12)$$

Substituting equation (12) into equation (11), we have

$$R_s(\tau) = \frac{1}{4\pi^2} \iint_{-\infty}^{\infty} R_H(\omega_k, \Delta\omega, \tau) X(\omega_k) e^{-is\omega_k} \delta(\omega_k - \omega_s) d\omega_k d\omega_s \\ = \frac{1}{4\pi^2} \int_{-\infty}^{\infty} R_H(\omega, 0, \tau) X(\omega) e^{-is\omega} d\omega \quad (13)$$

where $X(\omega)$ is the spectral density of the power of the input signal.

If a sine filter pulse of frequency ω_0 , amplitude A and width T_p is added at the input end of the system,

$$X(\omega) \approx \left(\frac{AT_p}{2}\right)^2 \left[\left(\frac{\sin(\omega - \omega_0)T_p}{(\omega - \omega_0)T_p} \right)^2 + \left(\frac{\sin(\omega + \omega_0)T_p}{(\omega + \omega_0)T_p} \right)^2 \right]$$

When T_p is sufficiently wide, the $(\sin x)/x$ function can be substituted by the δ function, thus

$$X(\omega) \approx \left(\frac{AT_p}{2}\right)^2 (\delta(\omega - \omega_0) + \delta(\omega + \omega_0)) \quad (14)$$

Substituting equation (14) back into equation (13) we obtain

$$\begin{aligned} R_s(r) &\approx \frac{1}{4\pi^2} \left(\frac{AT_p}{2}\right)^2 \int_{-\infty}^{\infty} R_N(\omega, 0, r) e^{-j\omega r} (\delta(\omega - \omega_0) + \delta(\omega + \omega_0)) d\omega \\ &= \frac{1}{4\pi^2} (AT_p)^2 R_N(\omega_0, 0, r) \cdot \cos \omega_0 r \end{aligned} \quad (15)$$

From the above analysis we see that changing different ω_0 and actually measuring $R_s(r)$, the correlation function $R_H(\omega_0, 0, r)$ of the system can be obtained from equation (15). When $R_H(\omega_0, 0, r)$ corresponding to $X(\omega)$ is a slow variant function of ω , $R_H(\omega, 0, r)$ in equation (13) can be taken out from the integral.

$$\begin{aligned} R_s(r) &\approx \frac{1}{4\pi^2} R_N(\omega_0, 0, r) \int_{-\infty}^{\infty} X(\omega) e^{-j\omega r} d\omega \\ &= \frac{1}{2\pi} R_N(\omega_0, 0, r) \cdot R_s(r) \end{aligned} \quad (16)$$

where ω_0 is the central frequency of the signal.

According to equation (7), we can write r in R_X as $r = (n - k)T + r_X$ and omit the periodic term $(n - k)T$; thus equation (16) becomes

$$R_s(r) \approx \frac{1}{2\pi} R_N(\omega_0, 0, r) \cdot R_s(r_x) \quad (17)$$

In general, regardless of the form of the signal used, from the actually measured correlation functions between pulses, we can obtain the system function $R_H(\omega, 0, r)$ that describes the characteristics of the communications channel from equation (17).

J. Some Explanations of the Characteristics of the Oceanic Sound Communications Channel

As everyone knows, the actual oceanic sound transmission channel is very complex; it is affected by random and uneven factors that have different physical mechanisms and thus the sound signals propagated along the communications channel follow multiple paths and are randomly variant in time and space. Therefore, the system function that describes the characteristics of the communications channel is also a random function of time and space variations; for example, $h = h(s, t, r)$, $H = H(i\omega, t, r)$. If h or H is a noninterfering pure random process (without any even portion), then the method of processing signals by matching the wave filter and the correlation between pulses will be completely ineffective. Conversely, if h and H are completely determined functions, this means the communications channel is determined; for example, the single path communications channel without distortion, the matching wave filter can reach its own most ideal processing increment of $10 \log(2W_1 T)$, (W_1 --front bandwidth of the receiver; T --length of signal). For the stable multiple communications channel, the correlation coefficient between pulses (compared to the large signal noise) will approach 1. But the actual situation is between the two, and the corresponding output is very closely related to the ocean situation, the ocean zone and the actual measuring time. The above shows the system function of the communications channel should consist of two parts. They are:

Completely interfering determined process--this is the "stable part" of the communications channel composed of the waveguide effect, stable sound velocity gradient, and stable oceanic flow. In addition, the determined process also includes the time-variant interference of the system function of the communications channel.

Noninterfering random time-variant process--this is the noninterfering portion of the system function of the communications channel composed of random undulations on the ocean surface, turbulence, and random motion of unevenly scattered objects. Therefore, the system's response function can be written as

$$h(s, r) = \sqrt{E_0} h_0(s) + \sqrt{E_1} h_1(s, r) + \sqrt{E_2} h_2(s, r) \quad (18)$$

where $\sqrt{E_0}$, $\sqrt{E_1}$, $\sqrt{E_2}$ are the uniformly weighted coefficients of the response function determined by the actual environment of the communications channel.

The first and second terms of the above equation respectively represent the stable portion of the communications channel and the interfering components of the time-variant response function of the communications channel. They are all completely interfering determined transformations of the communications channel. The third term represents the noninterfering random transformation of the communications channel. Thus, the correlation function between pulses of equation (4) can be written as:

$$R_s(t_1, t_2) = \iint_E E[(\sqrt{E_0}h_0(u_1) + \sqrt{E_1}\tilde{h}(u_1, t_1) + \sqrt{E_2}\tilde{h}(u_1, t_2))(\sqrt{E_0}h_0(u_2) + \sqrt{E_1}\tilde{h}(u_2, t_1) + \sqrt{E_2}\tilde{h}(u_2, t_2))] \cdot R_s(t_1 - u_1, t_2 - u_2) du_1 du_2 \quad (19)$$

whereas

$$\begin{aligned} E[\cdot] &= E[(\sqrt{E_0}h_0(u_1) + \sqrt{E_1}\tilde{h}(u_1, t_1))(\sqrt{E_0}h_0(u_2) + \sqrt{E_1}\tilde{h}(u_2, t_2))] \\ &= E_0h_0(u_1)h_0(u_2) + \sqrt{E_0E_1}(h_0(u_1)\tilde{h}(u_2, t_2) + h_0(u_2)\tilde{h}(u_1, t_2)) \\ &\quad + E_1\tilde{h}(u_1, t_1)\tilde{h}(u_2, t_2) \end{aligned} \quad (20)$$

When the process is wide-sense stationary, equation (20) becomes

$$\begin{aligned} E[\cdot] &= E_0h_0(u_1)h_0(u_2) + \sqrt{E_0E_1}(h_0(u_1)\tilde{h}(u_2) + h_0(u_2)\tilde{h}(u_1)) \\ &\quad + E_1R_s(u_1, u_2, \tau) \\ &= A(u_1, u_2) + E_1R_s(u_1, u_2, \tau) \end{aligned} \quad (21)$$

In the equation, $A(u_1, u_2)$ represents the sum of the first two terms, R_h is the correlation function of the response function of the communications channel. Substituting equation (21) into equation (19), and omitting the period term in the quantity of the correlation function of the input signal, we have

$$R_s(\tau) = \iint_E A(u_1, u_2)R_s(\tau_1 + u_1 - u_2)du_1 du_2 + \iint_E E_1R_s(u_1, u_2, \tau) \\ \cdot R_s(\tau_1 + u_1 - u_2)du_1 du_2$$

Appropriate adjustment of the delay time τ_x enables us to obtain

$$R_s(\tau) = \iint_E A(u_1, u_2)R_s(0)du_1 du_2 + \iint_E E_1R_s(u_1, u_2, \tau)R_s(0)du_1 du_2 \\ = B + R_s(\tau) \quad (22)$$

By normalizing $R_s(\tau)$ we can obtain the correlation coefficient $\rho_y(\tau)$ between pulses.

$$\rho_y(\tau) = b + r_s(\tau) \quad (23)$$

The constant b represents the "stable part" of the communications channel, for a definite transmitting and receiving position, it is unrelated to time. The term $r_s(\tau)$ is the contribution of the interfering part of the system function to the correlation coefficient between pulses.

Our measurements of the correlation coefficient $\rho_y(\tau)$ between pulses of the sound propagation channel and the reflection channel of a fixed target in shallow sea show that the so-called "stable part" does exist, because $\rho_y(\tau)$ lessens as τ increases and approaches a certain "stable value" b. Because of the random time-variant property of the communications channel, $\rho_y(\tau)$ drops as the correlative time increases, different dropping rates reflect different propagation characteristics, and thus it also shows that the method of correlation between pulses is an effective means to study the time-variant property of the communications channel. The following will introduce the method of measurement, give some results of actual measurements and give a preliminary analysis of the results.

II. Method of Measuring the Function $R_y(t_1, t_2)$ of Correlation Between Pulses and the Results of Measurements

1. Method of Measurement

We mentioned above that the system's correlation function $R_H(\omega, t_1, t_2)$ that represents the time-variant characteristics of the communications channel can be directly obtained from the system's output correlation function $R_y(t_1, t_2)$. In the following, we will introduce the method of measuring the $R_y(t_1, t_2)$ of the one-way transmission channel and the two-way echo channel.

(1) The measurements of $R_y(t_1, t_2)$ of one-way transmission are shown in Figure 3.

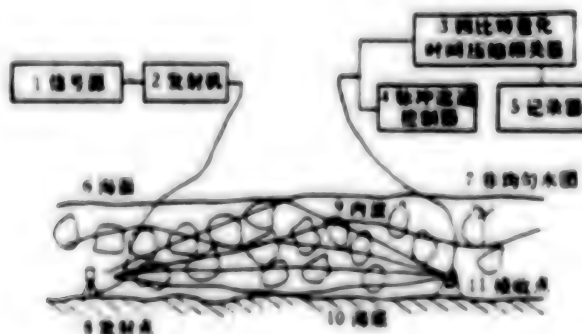


Figure 3. Block Diagram of Measuring $R_y(t_1, t_2)$ of a One-way Propagation Channel

Key:

1. Signal generator	6. Ocean surface
2. Transmitter	7. Inhomogeneous water cluster
3. Four-bit quantized compressed time-correlator	8. Transmitting point
4. Time gate	9. Interior wave
5. Recorder	10. Sea floor
	11. Receiving point

The transmitter is located on the transmission vessel. The transmission converter is placed at the bottom of the sea at a fixed location. For reception, an underwater base fixed at the bottom of the sea is used. The transmitter is controlled by the signal generator. A frequency modulated pulse FM 100 and a 32×20 coded phase modulated pulse are transmitted at intervals of $T = 5$ seconds. The pulse width is 640 ms. The pulsed signal travels via the underwater sound propagation channel to the 4-bit quantized linear time compressed correlator, and at the same time enters the pulse passage selection controller; the controller produces controlled square waves and groups the pulses received in order, every N number of pulses form a group, $n = 1, 2, \dots, N$. The correlator stores the first pulse received as a reference signal and correlates it with the second, third, ..., N th pulse received. In this way, we obtain R_{y11} , (t_1, t_2) , $R_{y12}(t_1, t_3)$, ..., $R_{y1N}(t_1, t_N)$ $i = 1, 2, \dots, k$ (i is ordering), $t_2 - t_1 = T$, $t_3 - t_1 = 2T$, ..., $t_N - t_1 = (N - 1)T$.

To eliminate the effect of amplitude undulations of the pulse, the correlation functions measured are converted to correlation coefficients, i.e.,

$$\rho_{nn}(t_1, t_2) = R_{nn}(t_1, t_2)/[Y_n(t_1)Y_n(t_2)] \quad (24)$$

where

$$Y_n(t_1) = \sqrt{R_n(t_1, t_1)} = \sqrt{R_{nn}(0)}$$

$$Y_n(t_2) = \sqrt{R_n(t_2, t_2)} = \sqrt{R_{nn}(0)}$$

The $\rho_{y11}, \rho_{y12}, \dots, \rho_{y1(N-1)}$ of each group are averaged according to their own quantity $i = 1, 2, \dots, k$.

$$\bar{\rho}_{nn} = \left(\frac{1}{k} \right) \sum_{i=1}^k \rho_{ni} \quad n = 1, 2, \dots, (N - 1) \quad (25)$$

to obtain the average value and the standard deviation for graphic representation.

(2) The measurement of $R_y(t_1, t_2)$ of the two-way echo wave is shown in Figure 4.

The method of measurement is basically the same as that for one-way transmission. The difference is that transmission and reception are both fixed at the bottom of the sea at the same underwater base. The echo comes from a fixed target at a definite distance in a definite position selected. When a fixed target at a distance of 16 cable lengths is selected, pulses are transmitted at intervals of $T = 10$ seconds; when a fixed target at a distance of 56 cable lengths is selected, $T = 20$ seconds.

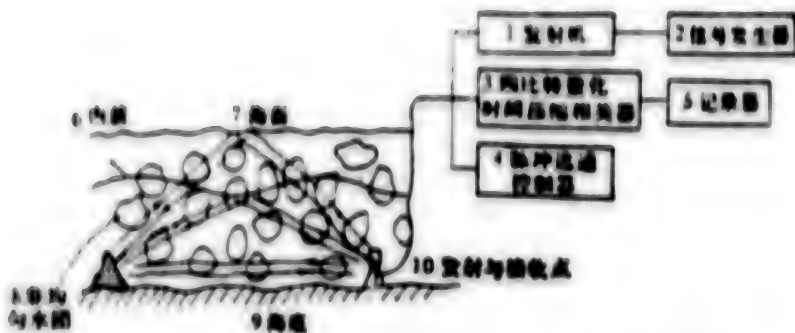


Figure 4. Block Diagram of Measuring $R_y(t_1, t_2)$ of a Two-Way Propagation Channel

Key:

1. Transmitter	6. Interior wave
2. Signal generator	7. Ocean surface
3. Four-bit quantized compressed-time correlator	8. Inhomogeneous water cluster
4. Time gate	9. Sea floor
5. Recorder	10. Transmitting and receiving point

2. Results and Analysis

Figures 5-7 show the curve of the correlation coefficients obtained by conversion from the actually measured $R_y(t_1, t_2)$. The actual conditions of measurement are labeled in Figure 5. "0" is the measured value, the solid line is the curve fitted by the least square method.

Statistical analysis of the data shows the correlation coefficients between the pulses of the transmission channel and the fixed target reflection channel basically attenuate exponentially as time increases. Also, the time-variant characteristic of the communications channel can be explained in general by the following illustrative Figure 8.

(1) For the determined ideal communications channel without noise interference, the correlation coefficients between pulses are unrelated to time, and $\rho_y(\tau) = 1$.

(2) For the determined communications channel (such as the stable and multiple path communications channel) with unrelated interference, the fixed correlative loss is produced by the noncorrelation of noise and mixed responses mixed in with the receiving signals; $\rho_y(\tau)$ does not change with time either, and surpasses a certain constant ($a + b$).

(3) For random time-variant communications channels possessing partial correlative characteristics, statistical analysis of a massive amount of data shows that the correlation coefficients between pulses drop exponentially as time increases; refer to equation (23).

$$\rho_y = ae^{-a\tau} + b$$

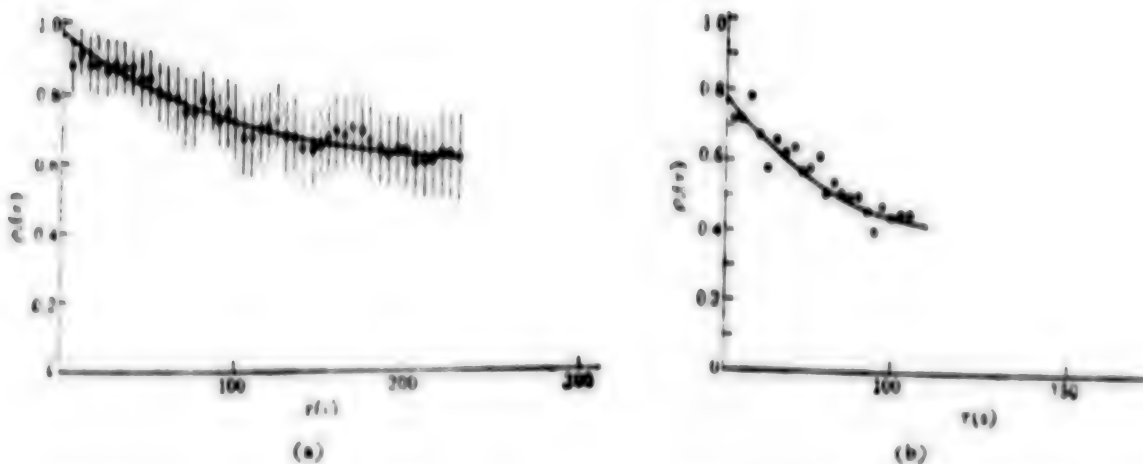


Figure 5. Time Variance of the Correlation Coefficients Between Signal Pulses in the Transmission Channel

(a) The form of the signal of the 79.4.27 shallow sea propagation experiment, the transmitting and receiving points were fixed at a distance of 4 nautical miles: FM 100, $t = 640$ ms.

o The measuring point is the arithmetic mean of 22 sets of data, and the standard deviation is labeled.

- The solid line is the fitted curve: $\rho_y(\tau) = ae^{-\alpha\tau} + b$ $a = 0.37$;
 $\alpha = 0.011$; $b = 0.6$

(b) The form of the signal of the 79.4.28 shallow sea propagation experiment, the transmitting and receiving points were fixed at a distance of 7 nautical miles: FM 100, $T = 640$ ms.

o The measuring point is the average value of 6 sets of data (standard deviation $\sigma_n < 0.15$).

- The solid line is the fitted curve: $\rho_{y_1}(\tau) = ae^{-\alpha\tau} + b$ $a = 0.436$;
 $\alpha = 0.016$; $b = 0.36$.

In the equation, a , α , b are constants and a , b are equivalent to E_0 and E_1 in equation (18). E_2 represents the scattered part of the communications channel satisfying the wide-sense stationarity uncorrelated scattering (WSSUS) condition (1). They are determined by the actual environmental conditions.

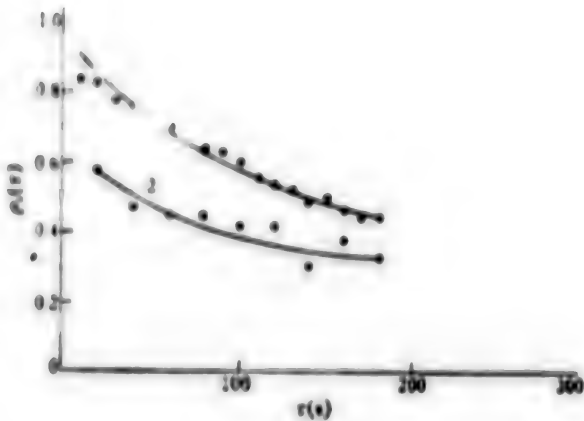


Figure 6. Variation of the Correlation Coefficients Between Pulses in the Two-way Communications Channel Along With Time

The 79.5.7 shallow sea fixed target reflection experiment FM 100, 640 ms

1. The target is 1.6 nautical miles from the base: The measured point "0" is the average value of 36 sets of data, the standard deviation is (0.13-0.18), the fitted curve is $\rho_y(\tau) = ae^{-\alpha\tau} + b$

$$a = 0.6; \alpha = 0.0104; b = 0.36$$

2. The target is 5.6 nautical miles from the base: The measured point "0" is the average value of 21 sets of data, the standard deviation is (0.13-0.21), the fitted curve is $\rho_y(\tau) = ae^{-\alpha\tau} + b$

$$a = 0.36; \alpha = 0.0141; b = 0.30$$

(4) It can be seen from the figures that the actual sound transmission channel also has the following outstanding characteristics:

- i. The first point of the actually measured correlation coefficient (i.e., the measured point corresponding to T seconds on the horizontal axis) drops by a larger scale, the latter neighboring points drop less in scale. We believe this is caused by the effects of random weighting of the signal by the communications channel and uncorrelated noise and mixed responses contained in the reference signal stored in the receiver.

- ii. It is also possible that a node Q exists. It can be derived from the first small point described in sections (2) and (4) that the time τ_0 corresponding to Q should be the correlated radius of the random interfering background and it is determined by the bandwidth of the interference.

- iii. Results of measurements show that $\rho_y(\tau)$ will approach a stable value b as time increases. This shows that regardless of how complex the transmission

characteristics of the communications channel are, there will always be a stable even part. R. Thiele (3) measured the scattering function 6 full days apart at two fixed points (at a distance of 1.6 nautical miles apart) on Fehmarn Island in the Baltic Sea, and the similarity of the results also explained this phenomenon.

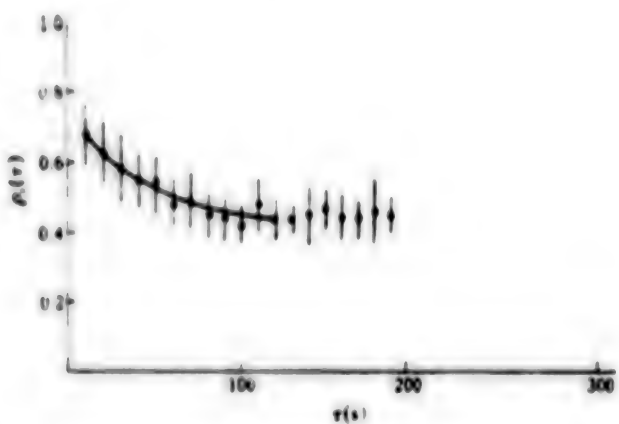
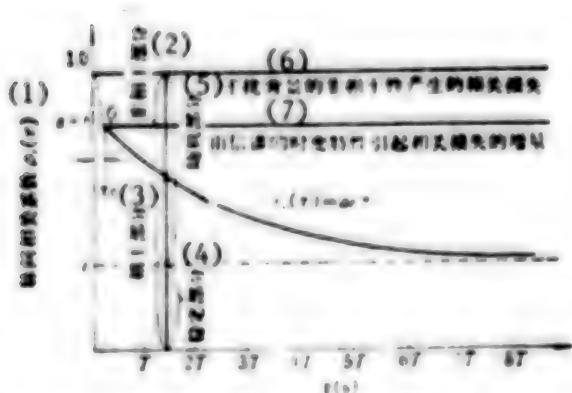


Figure 7. Variation of the Correlation Coefficients of Pulses in the Two-way Communications Channel Along With Time

The 79.5.11 shallow sea fixed target reflection experiment
Target was 1.6 nautical miles from the base, FM 100, 640 ms.

- δ The measured point is the average value of 20 sets of data, and the standard deviation is labeled.
- The solid line is the fitted curve.

$$\rho_y(\tau) = ae^{-\alpha\tau} + b \quad a = 0.34 \quad \alpha = 0.021 \quad b = 0.40$$



Key:

- (1) Correlation coefficient between pulses
- (2) Noninterfering part
- (3) Interfering part
- (4) Stable part
- (5) Random part
- (6) Correlative loss produced by noninterference of the interfering background
- (7) Increment of correlative loss caused by the time-variant characteristic of the communications channel

Figure 8. Illustrative Diagram of the Model of the Communications Channel

T is the interval of consecutive pulses; "o" is the average value of the measured points; the solid line is the curve fitted by the least square method,
 $y = ae^{-\alpha\tau} + b$.

III. Conclusion

1. Actual measurements show the oceanic sound transmission channel should consist of two parts, a determined transformation and a random transformation. The interfering part of the system function of the communications channel varies according to the differences in the actual ocean environment.
2. The method of correlation between pulses is a good method to study the random time-variant characteristics of underwater sound communications channels. The degree of the effect of the random time-variant part upon the transmission of sound in the communications channel can be expressed by the rate of exponential drop of $\rho_y(\tau)$ with time. The variations of the interfering and noninterfering parts of the communications channel can be directly obtained from measurements of the correlation coefficients.
3. The system function $R_H(t_1, t_2, \omega)$ of the communications channel can be obtained from the measurement of the coefficients of correlation between known signal pulses. This method can also be used directly to increase the reliability of underwater communications.

The above study of the oceanic sound transmission channel is preliminary and the data are insufficient; more profound work is still required.

The work benefited from a great deal of discussion with Comrades Huang Zengyang [7806 2582 2543] and Zhu Ye [2612 6851]. Comrades Sun Zeng [1327 1073], Sun Fuan [1327 4395 1344], Wei Xuehuan [7614 1331 3883], Zhou Wei [07.9 0251], and Zhou Guiqin [0719 2710 3830] participated in the experimental work.

REFERENCES

1. Laval, R., "Sound Propagation Effects on Signal Processing," in "Signal Processing," Proceedings of the NASI on Signal Processing (Academic Press, London 1973), 223. Translations on underwater acoustics (special edition on signal processing) (1975) 1.
2. Robert Laval, "Time-Frequency-Space Generalized Coherence and Scattering Functions," Aspects of Signal Processing, part I (1976), 69.
3. Thiele, R. "Measurement of the Weighting Function of the Time-Variant Shallow Water Channel," Aspects of Signal Processing With Emphasis on Underwater Acoustics NATO ASI Proceedings, part I, (1976), 109.

9296
CSO: 4008/367

PHYSICAL SCIENCES

SOUND WAVE PROPAGATION IN KAOLINITE SUSPENSION STUDIED

Beijing SHENGXUE XUEBAO [ACTA ACUSTICA] in Chinese No 3, 1981 pp 181-188

[Article by Tang Yingwu [0781 2019 0710] of the Acoustics Institute of the Chinese Academy of Sciences: "Propagation of Sound Waves in Kaolinite Suspensions"]

[Text] This article takes into consideration the effects of the mutual reaction of fluid dynamics and the mutual reaction of electrical forces in an acoustic field of suspended particles, revises the equivalent dynamic density equation and the motion equation of a suspension, and derives a more perfect expression of the effective density of a suspension. The consistency between the results and the experimental data is good.

I. Introduction

The question of sound propagation in suspensions has been the subject of study by many acoustics workers (1) because of its importance in application and its difficulty of treatment by mathematics (when using sound scattering). It is a question that has not yet been appropriately solved in sound propagation theory during the past 60 years. Past theoretical work mostly studied the velocity of sound and the absorption coefficient in suspensions separately; only a few articles have treated them together (2-4) (i.e., studying the question of sound propagation in suspensions), and the results obtained have neglected the mutual reactions of the suspended particles in the acoustic field. Such results are only appropriate for suspensions with a sufficiently low volume concentration. Experiments prove that when the volume concentration is greater than 0.8 percent (5), the mutual reactions of suspended particles in the acoustic field will emerge. Experiments by Urick (6) and Hampton (7) showed that the mutual reaction of suspended particles in an acoustic field is an important factor affecting sound propagation in a suspension. Therefore, in discussing sound propagation in a suspension, consideration must be given to the mutual reactions of suspended particles in the acoustic field.

*This article was received on 27 July 1979.

The mutual reactions of suspended particles in an acoustic field mainly include two types: the mutual reaction of fluid dynamics (8) and the mutual reaction of electrical forces (9) (for pure kaolinite particles). This article will omit the effects of the attenuation of scattering and the attenuation of thermal conductivity upon the propagation of sound, and will discuss the question of sound propagation in suspensions by considering the two types of mutual reactions described on the basis of Ament's (3) theory. The results obtained are compared with the experimental results. The theoretical and experimental results coincide very well.

II. Analysis of the Mutual Reactions of Suspended Particles in an Acoustic Field

Let us assume that the suspension consists of some electrically charged spherulitic particles of pure kaolinite of even size suspended in pure water (abbreviated water). When an acoustic field does not exist, the particles in the water are arranged in an equidistant cubic dot matrix. When there is an acoustic field, the wave line of the sound wave (the direction of propagation of the sound wave) is perpendicular to one side of this cubic dot matrix. To facilitate analysis, we number the particles and shade the plane of particles perpendicular to the wave line. The entire design is illustrated in Figure 1. From such an arrangement of particles, we can see the following:

1. When there is an acoustic field, the suspended particles on the same shaded plane are relatively stationary; therefore electrical forces do not exist between these particles.
2. In an acoustic field, the mutual reaction of fluid dynamics existing between one suspended particle and the neighboring one on the same shaded plane is the major reaction compared to the mutual reaction of fluid dynamics between these particles and other particles. This is because for each particle, the greatest interference of "water flow" surrounding it is exerted by the several neighboring particles. Because in an acoustic field, the "point mass" of water vibrates along the direction of sound propagation, thus when the wavelength of the sound wave in the suspension is very long compared to the linear dimension of the particle; the "water flow streamline" between particles on the same shaded plane contracts inward; this means that these particles exert the strongest resistance and friction on the flow of water, and thus, the mutual reaction of fluid dynamics between each particle and its neighboring particles is the strongest between those particles on the same shaded plane. Therefore, in this article we will only consider the mutual reaction of fluid dynamics between these particles.
3. In an acoustic field, the mutual reaction of electrical forces exists between the particle in the j th shaded plane and the several neighboring particles in the $(j - 1)$ th and $(j + 1)$ th shaded planes. In the following, we will analyze the electrical forces exerted on particle 0. When an acoustic field is not present, the distance between particle 0 and its closest neighboring particles 1 and $1'$ is d' ; the distance between particle 0 and its next closest neighboring particles 2, 4, 6, 8, $2'$, $4'$, $6'$ and $8'$ is $\sqrt{2} d$; the distance between particle 0 and the neighboring particles further away, 3, 5, 7, 9, $3'$, $5'$, $7'$ and $9'$ is $\sqrt{3} d$.

If we denote the electrical force exerting on particle 0 in the acoustic field defined by the particles 1-1' as f_0 , then from Figure 1 we know that the electrical forces exerted on particle 0 in the acoustic field defined by particles 2-2', 4-4', 6-6' and 8-8' are directly proportional to f_0 , and the electrical forces exerted on particle 0 in the acoustic field defined by 3-3', 5-5', 7-7' and 9-9' are also directly proportional to f_0 , only the proportional coefficients are different. Therefore, in the acoustic field, the electrical force F_0 on particle 0 is

$$F_0 = (1 + m_1 + m_2)f_0 \quad (1)$$

Here, m_1 and m_2 are two proportional coefficients to be determined.

The electrical force upon the other particles in the acoustic field is also F_0 .

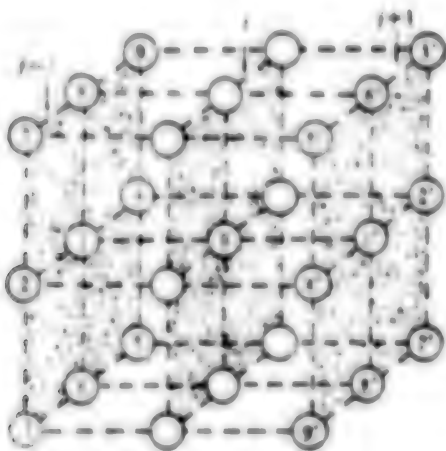


Figure 1. Suspended Particles Are Arranged in a Cubic Dot Matrix in a Stationary Body of Water

III. Effective Density

Ament used the following three equations (3) when he derived the effective density of a diluted suspension:

$$r = (1 - V_r)r_1 + V_r r_2 \quad (2)$$

$$\rho r = (1 - V_r)\rho_1 r_1 + V_r \rho_2 r_2 \quad (3)$$

$$(4/3)\pi r^3(\rho_2 r_2 - \rho_1 r_1) = (4/3)\pi r^3(S - \tau) \rho_1 \omega(r_2 - r_1) \quad (4)$$

where

$$r = \frac{1}{2} + \frac{9}{4\tau(\omega/2\mu)^{1/2}}$$

$$S = \frac{9}{4\tau(\omega/2\mu)^{1/2}} \left[1 + \frac{1}{\tau(\omega/2\mu)^{1/2}} \right]$$

ρ is the effective density of the suspension, v is the effective vibration velocity, $V_p (= 4 \cdot \pi r^3 N/3)$ is the volume concentration of the suspended particle, r is the radius of the particle, ω is the angular frequency, $n = n/n_1$, ρ_1 is the density of water, ρ_2 is the density of the particle, η is the viscosity coefficient of water, $i = \sqrt{-1}$, v_1 and v_2 represent the average vibration velocity of the water and particle in the suspension, N is the number of suspended particles in a unit volume. The time factor of the acoustic field is chosen as $e^{-i\omega t}$ (t is time), and is omitted.

Based on the arrangement of particles described in section two and the mutual reaction among the particles in the acoustic field, we let

$$k_0 d \ll 1 \quad (5)$$

thus, among equations (2) - (4), only equation (2) suits the present situation, and equations (3) and (4) must be revised before they can suit the present situation. This is because equation (2) is a continuous condition, and regardless of whether or not, it is always correct. Equation (3) is the equivalent dynamic density equation, and equation (4) is the equation of motion of suspended particles in the acoustic field. They are only correct when mutual reactions among suspended particles in an acoustic field do not exist. When mutual reaction among suspended particles in an acoustic field exists, they are not correct any more. In the following, we will consider the mutual reaction of suspended particles in an acoustic field to revise equations (3) and (4). The k_0 above is the phase shift constant (the real part of the propagation constant) of the suspension, d is the distance between the centers of two particles.

First we will discuss the revision of equation (3).

The equivalent dynamic density $(\rho v)_p$ in the suspension equals the sum of the motion $(\rho v)_p$ of the particles in a unit volume and the motion of water $(\rho v)_w$ is the unit volume, i.e.

$$\rho v = (\rho v)_w + (\rho v)_p, \quad (6)$$

where

$$(\rho v)_w = (1 - V_p) \rho_1 v_1 - P_v, \quad (7)$$

$$(\rho v)_p = V_p \rho_2 v_2 - N \int_{r_1}^{r_2} F_r \cdot dr + P_v, \quad (8)$$

Here, P_v is the viscous motion density, the density causing the loss in the motion of water due to viscous drag between the water and particles; $N \int_{r_1}^{r_2} F_r \cdot dr$ is the motion density of electrical force, the density causing the loss in the motion of the particles due to repulsive forces in the acoustic field. For the arrangement of particles in Figure 1, when equation (5) is valid, McCann (9) has already found

$$F_r = -\beta d^2 \frac{dv}{dr} = \frac{4}{3} \pi r^3 \rho_1 \rho_2 V_p^2 \frac{dV_p}{dr} \quad (9)$$

Therefore F_e in equation (1) can be expressed as

$$F_e = \frac{4}{3} \pi r^3 \rho_1 (1 + m_1 + m_2) P V_i^{1/2} \frac{d\bar{v}_2}{dt} \quad (10)$$

where P is a constant, \bar{v}_2 is the instantaneous vibration velocity of the particle.

Substituting equation (10) into equation (8) and when $t = t_1$, $\bar{v}_2 = 0$, when $t = t_2$, $\bar{v}_2 = v_2$, thus

$$(\rho v)_e = \rho_1 v_1 (\sigma - HV_i^{1/2}) + P, \quad (11)$$

where $\sigma = \rho_2/\rho_1$, $H = (1 + m_1 + m_2)P$.

Substituting equations (7) and (11) into equation (6), we obtain the equivalent dynamic density equation in the suspension:

$$\rho v = (1 - V_r) \rho_1 v_1 + V_r \rho_1 (\sigma - HV_i^{1/2}) v_1 \quad (12)$$

Now we will discuss the revision of equation (4).

Because of the presence of mutual reactions of fluid dynamics between suspended particles in the acoustic field, the vibration velocity of the particles relative to water ($v_2 - v_1$) will increase by ψ times. Thus, equation (4) should be revised as

$$\frac{4}{3} \pi r^3 \omega (\rho_2 v_2 - \rho_1 v_1) = \frac{4}{3} \pi r^3 (S - i\tau) \rho_1 \psi \omega (v_2 - v_1) \quad (13)$$

Here, ψ is a function of V_c , called the mutual reaction function of fluid dynamics between suspended particles in an acoustics field. If only the mutual reaction of fluid dynamics occurring between a particle and its neighbor on the same shaded plane is taken into consideration, we have (8)

$$\psi = \left[1 - \frac{3}{4} \left(\frac{6V_c}{\pi} \right)^{1/2} - \frac{1}{4} \left(\frac{6V_c}{\pi} \right) \right]^{-1} \quad (14)$$

Also, because of the mutual reaction of electrical forces among suspended particles in the acoustic field, the contribution of electrical forces must also be added to the left side of equation (13). Thus, equation (4) is finally revised to:

$$i((\sigma - HV_i^{1/2})v_1 - v_1) = (S - i\tau)\psi(v_2 - v_1). \quad (15)$$

Simultaneously solving equations (2), (12) and (15) yields the ρ expression for the effective density of the suspension:

$$\rho = \rho_1 + \frac{i\rho_1(\sigma - 1 - HV_i^{1/2})^2 V_i^{1/2} (1 - V_r)}{4S - i[\psi r + \sigma - HV_i^{1/2} - V_i(\sigma - 1 - HV_i^{1/2})]}, \quad (16)$$

where $\rho_1 = (1 - V_r)\rho_1 + V_r \rho_1$.

Of course, when $H = 0$ (or $P = 0$), equation (16) is reduced to the expression (19) in Reference (10). When $\psi = 1$ and $H = 0$, equation (16) reduces to the results of Ament, or degenerates to equation (27) in Reference (11).

IV. Propagation Constant

Because we do not consider the effects of sound attenuation caused by heat conduction upon the propagation of sound in a suspension, the coefficient K of absolute heat compression in the suspension takes real values (4), and its expression is

$$K = (1 - V_c) K_1 + V_c K_2,$$

here K_1 and K_2 are the coefficients of absolute heat compression of the water and the pure kaolinite particle. Substituting equation (16) into the expression

$$k = \omega(K\rho)^{1/2} \quad (17)$$

yields the sound propagation constant k in the suspension.

In our case, the quantity $\rho(\sigma - 1 - HV_c^2)^2 V_c(1 - V_c)$ is much smaller than 1; therefore the real part $\text{Re}(\rho)$ of ρ is much larger than ρ the imaginary part $\text{Im}(\rho)$ of ρ , i.e., $\text{Re}(\rho) \gg \text{Im}(\rho)$; thus equation (17) can be simplified to

$$\begin{aligned} k &\approx \omega(K \text{Re}(\rho))^{1/2} [1 + i \text{Im}(\rho)/2 \text{Re}(\rho)] \\ &= k_0 + i\alpha, \end{aligned} \quad (18)$$

From k_0 we can obtain the sound phase velocity c_p in the suspension:

$$c_p = 1/(K \text{Re}(\rho))^{1/2}; \quad (19)$$

α is the sound amplitude absorption coefficient in the suspension; its expression is

$$2\alpha = \omega \left[\frac{K}{\text{Re}(\rho)} \right]^{1/2} \frac{\rho V_c (1 - V_c)(\sigma - 1 - HV_c^2)^2 \phi S}{(\phi S)^2 + Q^2}, \quad (20)$$

where

$$\begin{aligned} \text{Re}(\rho) &= \rho - \frac{V_c (1 - V_c)(\sigma - 1 - HV_c^2)^2 Q}{(\phi S)^2 + Q^2} \\ Q &= \phi S + \sigma - HV_c^2 - V_c(\sigma - 1 - HV_c^2). \end{aligned}$$

V. The Expressions of the Sound Phase Velocity and the Absorption Coefficient

With equations (19) and (20), it is possible to theoretically calculate the sound phase velocity and absorption coefficient in a suspension, but it is not possible in the actual situation because the constant H is not yet determined. In the following, we have utilized the experimental data from Urick (6) to determine the value of the constant H . When the frequency is 1 megahertz, Urick measured the dependent relationship of the sound absorption coefficient upon the particles' volume concentration in the pure kaolinite suspension; the measured results are shown in Figure 2. The physical parameters of the suspension are: $\rho_1 = 1.00 \text{ g/cm}^3$, $\rho_2 = 2.65 \text{ g/cm}^3$, $r = 4.70 \times 10^{-5} \text{ cm}$, $u = 0.01 \text{ cm}^2/\text{s}$ (equivalent to 20°C in temperature), $c_p \approx 1.52 \times 10^5 \text{ cm/s}$, $\omega = 2\pi \times 10^6$. We selected various values for H and together with the above parameters we substituted them into expression (20) for numerical calculation. We discovered in the results that the $a-V_c$ characteristic curve (the solid line in Figure 2) calculated when $H = 0.7$ and the experimental data coincide well (except beyond the range $V_c > 0.35$). In this way, we determined that $H = 0.7$. At this time, the expressions (19) and (20) of the sound phase velocity and absorption coefficient in the suspension can be written as

$$C_s = \left\{ K \rho_s - \frac{K V_s (1 - V_s)(\sigma - 1 - 0.7V_s^{1/3})^2 (\phi r + \sigma - 0.7V_s^{1/3} - V_s(\sigma - 1 - 0.7V_s^{1/3}))}{\phi^2 S^2 + (\phi r + \sigma - 0.7V_s^{1/3} - V_s(\sigma - 1 - 0.7V_s^{1/3}))^2} \right\}^{-1/2} \quad (21)$$

$$2a = \omega \left(\frac{K}{\rho_s} \right)^{1/2} \frac{\rho_1 V_s (1 - V_s)(\sigma - 1 - 0.7V_s^{1/3})^2 S \phi}{\phi^2 S^2 + (\phi r + \sigma - 0.7V_s^{1/3} - V_s(\sigma - 1 - 0.7V_s^{1/3}))^2} \quad (22)$$

Ordinarily, $(\phi r + \sigma - 0.7V_s^{1/3}) \gg V_s(\sigma - 1 - 0.7V_s^{1/3})$, thus expressions (21) and (22) can be simplified to

$$C_s \approx \left\{ K \rho_s - \frac{K V_s (1 - V_s)(\sigma - 1 - 0.7V_s^{1/3})(\phi r + \sigma - 0.7V_s^{1/3})}{\phi^2 S^2 + (\phi r + \sigma - 0.7V_s^{1/3})^2} \right\}^{-1/2} \quad (23)$$

$$2a \approx \omega \left(\frac{K}{\rho_s} \right)^{1/2} \frac{\rho_1 V_s (1 - V_s)(\sigma - 1 - 0.7V_s^{1/3})^2 \phi S}{(\phi S)^2 + (\phi r + \sigma - 0.7V_s^{1/3})^2}. \quad (24)$$

Expression (24) is the same as formula (16) in Reference (8).

When the volume concentration of the particle in the suspension is very low (i.e., when $V_c \ll 1$), expressions (21) and (22) can be further simplified to

$$C_s = (K \rho_s)^{-1/2} = C_w \quad (25)$$

$$2a \approx \frac{\omega}{C_s} V_s \frac{(\sigma - 1)^2 S}{S^2 + (\sigma + r)^2} \quad (26)$$

Expression (25) is the famous Wood formula, while equation (26) is the same as the Lamb-Urick (6) formula.

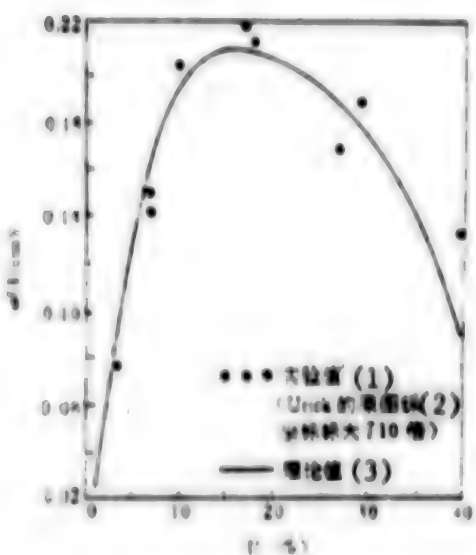


Figure 2. The Dependent Relationship of α Upon V_c at a Frequency of 1 MHz, and the Determination of the Value of the Constant P

Key:

- (1) Experimental values
- (2) (In Urick's original graph, the vertical coordinates were 10 times larger)
- (3) Theoretical values

Expression (23) shows that the sound phase velocity in the suspension is a function of frequency. Expression (24) shows that the sound absorption coefficient in the suspension is not directly proportional to the linear equation of frequency. These results can be explained by the Kramers-Kronig dispersion relationship (12) in quantum theory.

In some natural coagulated suspensions, the dependent relationship of the sound phase velocity and the absorption coefficient upon frequency (for example, in clay sediments on the sea floor, C_p and frequency are unrelated (13), α is directly proportional to the linear equation of frequency) (13, 14) cannot be explained by the theoretical results described above. This shows that the results of this article cannot be used for coagulated suspensions. The main mechanism of sound absorption in a coagulated suspension is internal friction of the suspension (10).

VI. Comparison of Theory and Experiment

Within the range of $0 < V_c < 0.4$ of volume concentration of particles, Hampton (7) measured the dependent relationship of the sound phase velocity in the pure kaolinite suspension (frequency is between 50 kilohertz and 20 kilohertz) and the absorption coefficient (frequency is 100 kilohertz) upon the volume concentration of the particles. Within the frequency range of $10-10^3$ kilohertz, Hampton also measured the dependent relationship of the sound absorption coefficient in the pure kaolinite suspension upon frequency; the corresponding volume

concentrations were 0.30 and 0.37. The results of the measurements are shown in Figures 3-5. The black dots in the diagrams are the experimental data of Hampton, the solid lines are the theoretical values of this article, the dotted lines are the theoretical values of Ament. The percentages in Figure 5 are the volume concentrations of the particles. The physical parameters of the pure kaolinite suspension used were: $\rho_1 = 1.00 \text{ g/cm}^3$, $\rho_2 = 2.71 \text{ g/cm}^3$, $r = 1.20 \times 10^{-6} \text{ cm}$, $\mu = 0.01 \text{ cm}^2/\text{s}$, $K_1 = 4.44 \times 10^{-12} \text{ cm}^2/\text{dyn}$, $K_2 = 1.00 \times 10^{-12} \text{ cm}^2/\text{dyn}$.

Under Hampton's experimental conditions, equation (5) is satisfied.

It can be seen from Figures 2-5 that:

1. Consistency of the theoretical results of this article and the experimental data is very good. The theoretical results of this article are much better than the theoretical results of Ament.
2. There is a visible frequency scattering effect in the pure kaolinite suspension, and the velocity of sound increases as the frequency increases.
3. The sound absorption coefficient in the pure kaolinite suspension is not a linear function of the volume concentration of the particles; when the volume concentration of particles is about equal to 0.17, the absorption coefficient has a maximum value.
4. Within a frequency range of 10 to 1,000 kilohertz, the sound absorption coefficient in the pure kaolinite suspension discussed is directly proportional to the nth degree equation of frequency; the degree n satisfies the inequality:

$$1.14 < n < 1.82.$$

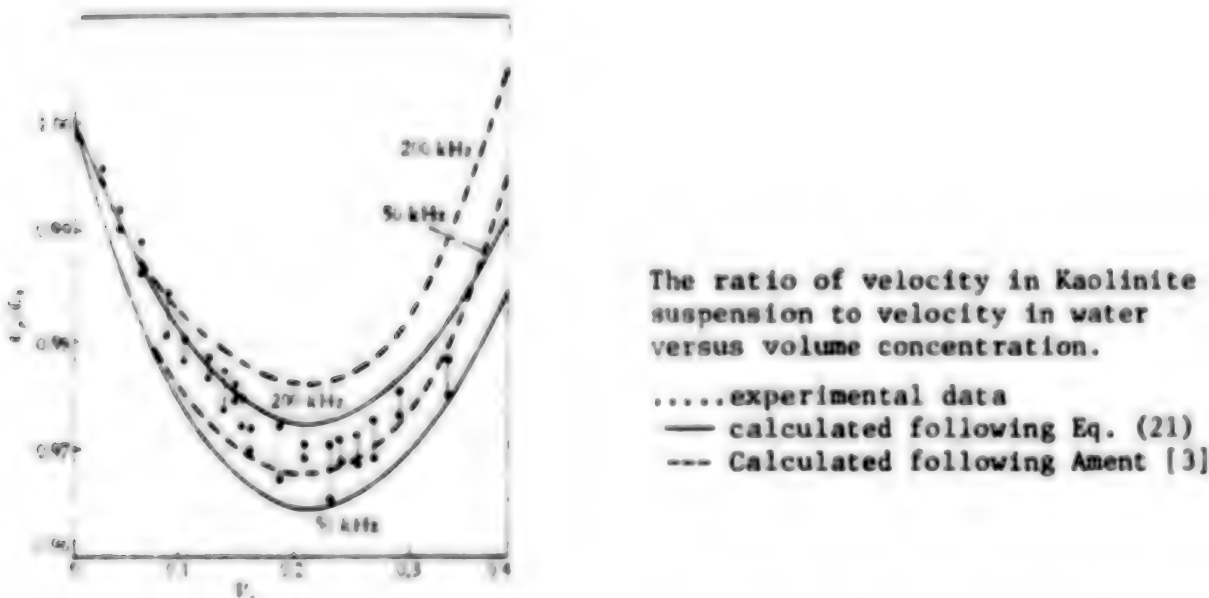


Figure 3. The Dependent Relationship of C_p/C_1 Upon V_c , a Comparison of Theory and Experiment

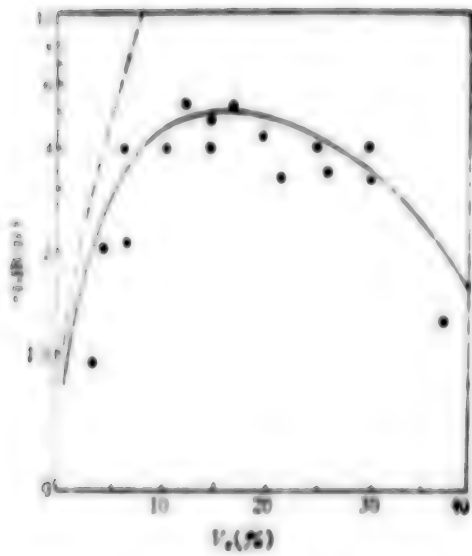


Figure 4. The Relationship of α to V_c at a Frequency of 100 kHz, Comparison of Theory and Experiment

Dependence of absorption coefficient (in decibels perfoot) on volume concentration at 100 kHz.

- ... experimental data
- calculated following Eq (22)
- - calculated following Ament

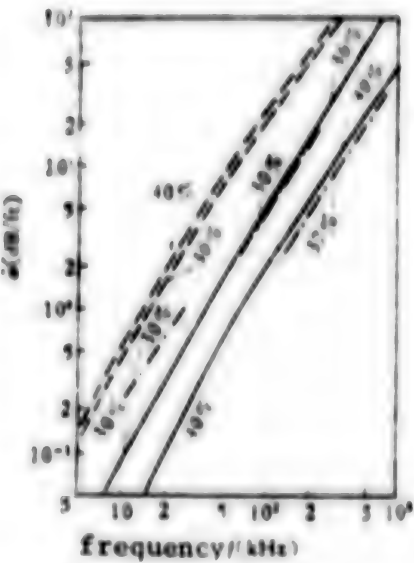


Figure 5. Comparison of the Theoretical and Experimental Relationship of α to Frequency

Absorption coefficient as a function of frequency. The volume concentration of each kaolinite suspension is noted on each graph.

- ... experimental data
- calculated following Eq (22)
- - calculated following Ament

VII. Discussion

In Reference (8) we only considered the mutual reaction of electrical forces between the particles in the j th shaded plane and the closest neighbors in the $(j-1)$ th and the $(j+1)$ th shaded planes, and we neglected the mutual reaction of electrical forces between that plane and the next closest and further neighbors. Actual calculations show that m_1 and m_2 are numbers close to 1, and their contribution cannot be ignored. But because the value of P in Reference (8) was determined by experimental data, this shows that in Reference (8), m_1 and m_2 have already been unobtrusively added, i.e., the P determined in Reference (8) is numerically equal to H determined in this article. Although the value of P determined in Reference (8) was larger, equation (16) of Reference (8) is still effective.

Experiments by Urick pointed out that the theory of this article can be applied within a volume concentration range of $0 < V_c < 0.35$ (see Figure 2), while the experimental results of Hampton indicated that the suitable range of the theory of this article can be even wider, i.e., it is applicable within the range of $0 < V_c < 0.4$. It seems that theoretical and experimental research in the theory of sound propagation in suspensions of a high concentration range is still worth continuing.

REFERENCES

1. Allegra, J. R., et al, "Attenuation of Sound in Suspensions and Emulsions: Theory and Experiments," *J. Acoust. Soc. Am.*, 51(1972), 1545-1564.
2. Urick, R. J., et al, "The Propagation of Sound in Composite Media," *J. Acoust. Soc. Am.*, 21(1949), 115-119.
3. Ament, W. S., "Sound Propagation in Gross Mixtures," *J. Acoust. Soc. Am.*, 25(1953), 638-641.
4. Ahuja, A. S., "Wave Equation and Propagation Parameters for Sound Propagation in Suspensions," *J. Appl. Phys.*, 44(1973), 4863-4868.
5. Wei Rongjue [7614 2837 3635], Zhang Shuyi [1728 3219 0308], "Absorption of Ultrasonic Waves in a Suspension (Water)," *WULI XUEBAO (Journal of Physics)*, 21(1965), 1061.
6. Urick, R. J., "The Absorption of Sound in Suspensions of Irregular Particles," *J. Acoust. Soc. Am.*, 20(1948), 283-289.
7. Hampton, L. D., "Acoustic Properties of Sediments," *J. Acoust. Soc. Am.*, 42(1967), 882-890.
8. Tang Yingwu [0781 2019 0710], "Absorption of Sound Waves in Gross Suspensions," *JOURNAL OF THE ZHONGSHAN UNIVERSITY (Natural Sciences Edition, 1977)*, No 4, 52-59.
9. McCann, C., "Compressional Wave Attenuation in Concentrated Clay Suspensions," *ACUSTICA*, 22 (1969-70), 352-356.
10. Tang Yingwu [0781 2019 0710], "Propagation of Elastic Waves in Sediments," *GEOPHYSICS JOURNAL*, 18 (1975), 269-278.
11. Ahuja, A. S., "Effect of Particle Viscosity on Propagation of Sound in Suspensions and Emulsions," *J. Acoust. Soc. Am.*, 51(1972), 182-191.
12. Horton, Sr, C. W., "Dispersion Relationships in Sediments and Sea Water," *J. Acoust. Soc. Am.*, 55(1974), 547-549.
13. Hamilton, E. L., "Compressional Wave Attenuation in Marine Sediments," *GEOPHYSICS*, 37(1972), 620-646.
14. McLeroy, E. G., et al, "Sound Speed and Attenuation, From 15 to 1,500 kHz, Measured in Natural Sea Floor Sediments," *J. Acoust. Soc. Am.*, 44(1968), 1148-1150.

9296
CSO: 4008/367

ELECTRIC SHOCK THERAPY USED IN EPILEPSY TREATMENT

Clinical Data

Beijing ZHONGHUA SHENJING JINGSHENKE ZAZHI [CHINESE JOURNAL OF NEUROLOGY AND PSYCHIATRY] in Chinese No 1, 1981 pp 42-44

[Article by Wang Zucheng [3769 4371 2110] and Yu Shicai [0060 0013 2088] of the Shanghai Psychiatric Hospital, Ma Huiying [7456 1979 3853] of Guizhou 304 Hospital, and Song Zhanping [1345 1413 1627] of the Shanghai City Nanshi Ward Psychiatric Hospital: "Clinical Study of Electric Shock Therapy of Epileptic Mental Disturbances; Analysis of 32 Cases"]

[Text] Electric shock therapy is a method of treating mental disturbance by artificially inducing an epileptic reaction in order to better pinpoint symptoms of epileptic mental disturbance through electric shock treatment and thus effectively and rapidly control the symptoms and improve the effectiveness of treatment of mental disturbance accompanied by epileptic reaction. We have gathered for clinical analysis our hospital's information over the past 21 years on the use of electric shock to treat epileptic mental disturbances.

I. Source of Information

Between August 1958 and June 1979, a total of 490 cases of epileptics were admitted into our hospital. Electric shock treatment was used to treat epileptic mental disturbances in 32 of these cases, or 6.5 percent of the epileptics hospitalized. In three cases, the patients were given repeated electric shock treatment when they were hospitalized again. Except in two cases, the nature of the epilepsy was recurring epilepsy.

II. Analysis of Information

1. General information: (1) There were 19 males and 13 females. Their ages ranged from 16 to 52 years old. In 7 cases the patients were 16 to 20 years old; in 13 cases the patients were 21 to 30 years old; in 8 cases the patients were 31 to 40 years old; and in 4 cases the patients were over 41 years old. (2) The duration of hospitalization varied from 7 days to 14 years. There were 28 case-times in which hospitalization was less than half a year. (3) The history of the disease varied from 4 days to 20 years. In 17 case-times the case history was less than 5 years; in 8 case-times it was 5 to 10 years; in 8 case-times, 10 to

15 years; and in 2 case-times, 15 to 20 years. (4) In 18 case-times, mental disturbance occurred within 1 year; in 15 case-times, mental disturbance occurred within 1 to 5 years; in 2 case-times, mental disturbance occurred within 5 to 20 years. In 18 of the 35 case-times, epileptic reactions occurred simultaneously with mental disturbance; for 16 instances, epilepsy occurred before mental disturbance; and in 1 case mental disturbance occurred before epileptic reaction. (5) Clinical types of epilepsy and mental disturbances: There were 13 case-times (12 cases) of schizophrenic epileptic mental disturbance, 7 case-times (7 cases) of epileptic psychomotor reactions, 7 case-times (7 cases) of major and minor epilepsy accompanied by schizophrenia, 5 case-times (3 cases) of epileptic personality disturbance, 2 case-times (2 cases) of mental disturbance caused by recurrent epilepsy, and 1 case-time (1 case) of major epileptic reaction accompanied by menopause psychosis. (6) Combined medication: Except for 1 case, electric shock treatment was given in the remaining 34 case instances simultaneously with antipsychotic medication during hospitalization. The types of medical drugs included chlorpromazine, perphenazine, tardanum, fluoropiperidyl alcohol, reserpine, trifluorazine, fluoroperphenazine, and lithium carbonate. Daily dosage for treatment was within the commonly administered dosage.

In 30 instances, electric shock therapy was combined with antiepileptic medication. Phenytoinum natricum was administered in 27 instances, phenobarbital was administered in 26 instances (in 21 instances, phenytoinum natricum and phenobarbital were administered in combination), primidonum was administered in 3 instances, meprobamatum was administered in 2 instances, and librium was administered in 1. In 5 instances, medication and shock therapy were not combined.

2. Analysis of information on electric shock treatment: (1) Electric voltage, electric current intensity, and duration of electric shock treatment: In the group of cases treated in combination with antiepileptic medication, the threshold value of treatment of most cases was high, while in the group of cases treated without combination with antiepileptic medication, the threshold value was equal to the threshold value of ordinary treatment of psychosis. (2) The interval between electric shock treatments and total number of treatments: In 16 instances, the interval of treatment was basically according to the usual interval of treatment--i.e., at the beginning, treatment was given two or three times a week, totaling five to eight times, and then treatment was changed to one or two times a week; 9 to 12 times of treatment were counted as one course of treatment. In another 15 instances, the treatment interval was often over 1 week, and there was no fixed pattern. In the other four cases, statistics were unavailable because the record of treatment was not detailed or the records were lost. In the total number of treatments, 6 treatments or fewer were given in 17 instances, 6 to 12 treatments were given in 13 instances, and more than 12 treatments was given on only one occasion; there were 4 other cases with incomplete records. The total number of treatments was similar to the number given when treating schizophrenia. (3) The relationship between electric shock treatment and epileptic reaction: We marked out the month before electric shock treatment began and the month following the end of treatment. During this period, epileptic reactions occurred simultaneously with the administration of electric shock treatment in 13 instances. During this period there were 22 instances in which there was electric shock treatment without its being accompanied by epileptic reaction. Among the 13 instances in which electric shock treatment was given at the same time as the occurrence of epileptic reactions, the treatment stimulated an increase in epileptic reactions

in 4 instances, and the treatment produced a decrease in epileptic reactions in 9 instances.

3. Analysis of the effects of electric shock therapy: (1) The effectiveness of treatment of various clinical types: Electric shock therapy was effective in 5 of 7 instances of psychomotor epileptic reaction, in 9 of the 13 instances of schizophrenic epileptic psychosis, in 4 of the 7 instances of major or minor epileptic reactions accompanied by schizophrenia, and in 2 of the 5 instances of epileptic personality disturbance. It was effective in one of the three instances of other epileptic mental disturbance or epileptic reactions accompanied by psychosis. Of the 35 case-times, it was effective in 21 instances, and so the total percentage of effectiveness was 60 percent. It was ineffective in both of the cases of recurrent epilepsy. (2) The effectiveness of treatment of individual psychotic symptoms: Electric shock therapy was effective in the treatment of symptoms of speaking to oneself, disorderly behavior, melancholia, disorganized thought, excitability and being easily angered, impulsive destruction, and delusion, as shown in the accompanying table. (3) The relationship between effectiveness of treatment and the course of epilepsy and psychosis: There were 18 instances of simultaneous occurrence of epilepsy and mental disturbance; treatment was effective in 13 of these, or 72.2 percent. There were 16 cases of epilepsy before the occurrence of mental disturbance; treatment was effective in 8, or 50.0 percent. There was one instance in which mental disturbance was followed by epileptic reaction, and treatment was ineffective. It seems that the effectiveness of treatment of the first type of cases was better than in the second type of cases, while there was only one case in the third type and judgment could not be made. (4) Relationship between effectiveness of treatment and the frequency of treatment: In 9 instances, effectiveness of the treatment occurred within 6 treatments, while in 8 instances the treatment was ineffective; thus the percentage of effectiveness was 52.9 percent (9/17 case-times). In 10 instances, effectiveness occurred after 7 to 12 treatments, while in 3 instances the treatment was ineffective; thus the percentage of effectiveness was 76.9 percent (10/13 case-times). The percentage of effectiveness is higher [when the frequency of treatment is greater] than otherwise.

Accompanying Table. Effectiveness of Electric Shock Therapy in the Treatment of Psychotic Symptoms

Key:

- A. Psychotic symptoms
- B. Case-times
- C. Effective case-times
- D. Percentage of effectiveness
- 1. Speaking to oneself
- 2. Disorderly behavior
- 3. Melancholia
- 4. Disorganized thought
- 5. Excitability and being easily angered
- 6. Impulsive destruction
- 7. Delusion
- 8. Personality changes
- 9. Emotional incoordination
- 10. Phonism
- 11. Somnolent state

(A)	(B)	(C)	(D)	(A)	(B)	(C)	(D)
精神病状	例次	有效例次	有效率%	精神病状	例次	有效例次	有效率%
(1) 言語	15	14	93.3%	妄想	14	11	78.6
(2) 行为失常	23	20	87.0%	情感改变	9	7	77.8
(3) 性格改变	14	12	85.7%	情感不协调	7	5	71.4
(4) 思维杂乱	11	9	81.8%	幻(10)听	10	7	70.0
(5) 兴奋易激怒	16	13	81.2%	朦胧状态	8	5	62.5
(6) 情感波动	20	16	80.0%	(11)			

4. Side effects after electric shock therapy: In 35 case-times, following some 250 electric shock treatments, there were 6 cases (7 case-times) that showed side effects, or 20 percent of the total case-times. Side effects were manifested as follows: In four cases, major epileptic reactions occurred frequently after two electric shock treatments. In one case, semiconsciousness, excitation, and a manic state accompanied by refusal to eat occurred after six electric shock treatments; these effects persisted for 4 days, and then a major epileptic reaction occurred and the condition improved. In 1 case, a stiffness state occurred after 10 electric shock treatments and the condition improved later by itself.

III. Discussion

There have already been reports on the use of tic to treat epileptic reactions. The reaction threshold of epilepsy can be increased in epileptic patients who have used certain medicines (such as metrazol) to cause convulsions. The reports have also mentioned frequent death due to recurrent epilepsy of "combined epileptic and psychotic symptoms." If this type of reaction can be induced by man artificially, the duration of mental disturbance of the patients can be greatly shortened. Therefore, Kalinowsky believed: Artificially induced epilepsy serves a protective function in automatic epilepsy. If antiepileptic drugs still cannot control epileptic reactions, electric shock can be used to suppress such reactions. He also pointed out: Incomplete epileptic reactions can be terminated by one or two automatic or artificially induced epileptic reactions. Gerletti mentioned that the use of electric shock therapy to treat epileptic patients can suppress automatic epileptic reactions for a longer period of time. Some writings have also pointed out that the use of electric shock therapy to treat epileptic mental disturbance, psychomotor reactions, schizophrenic epileptic mental disturbance, and somnolent states has a definite effect, and it can check some major epileptic reactions and emotional disturbance and improve the condition. Ouchi et al believed: "Electric shock treatment of schizophrenic epileptic delusion symptoms 4 to 10 times has a definite effect, and it can also eliminate hallucinations, but there are also ineffective cases."

From our indications, the most suitable types of epileptic mental disturbance for electric shock treatment are: psychomotor reactions, personality disturbance, schizophrenic mental disturbance, and major and minor epilepsy accompanied by schizophrenic patients. The effectiveness is always 60 percent and close to the percentage of effectiveness (66 percent) in the treatment of schizophrenia by electric shock therapy mentioned by Cornelio. In 13 cases, major epilepsy occurred within the period from 1 month before to 1 month after electric shock treatment. Of these, there were nine cases (69.2 percent) in which electric shock treatment caused a reduction in epileptic reactions; this is consistent with reports that electric shock therapy can suppress major epileptic reactions. But we should also note that in a few cases (four cases, 30.8 percent), treatment was terminated because of more frequent reactions. In addition, we also note a total of six cases of transient semiconsciousness, excitation and manic activity, and stiffness state which subsided and the condition of the patients improved without any visible after effects. Thus, electric shock therapy is a relatively safe method of treating automatic epileptic mental disturbance.

In 32 cases (35 case-times), 30 were given antiepileptic medication simultaneously and the treatment threshold values were mostly higher. The treatment threshold value in the five instances in which medication was not given was equal to the threshold values of electric shock treatment of other kinds of psychosis. Therefore, epilepsy does not increase the treatment threshold value, but the threshold values increased only after taking antiepileptic medicines.

In the method of electric shock therapy for treatment of epileptic mental disturbance, the interval of treatment and the total frequency of treatment are basically the same as those in ordinary electric shock therapy. Although nearly one-half (48.5 percent) of the cases in the data received a total of six or fewer treatments, the effectiveness rate was only 52.9 percent. The effectiveness of treatment was 76.9 percent for cases treated 7 to 12 times, far higher than those cases treated six or fewer times. It can be seen that to obtain the maximum result of treatment, the total number of customary electric shock treatments is required.

The mechanism of electric shock therapy for treating epileptic mental disturbance has been explained by Kalinowsky: Electric shock treatment can temporarily increase the tic threshold value. From this we can infer that electric shock increases the discharge threshold value manifested as psychotic symptoms and thus causes the psychotic symptoms to disappear. Because we still are unable to explain epilepsy and the mental disturbance caused by it perfectly, and because the mechanism of electric shock therapy is not completely clear, we can only make such an inference.

Clinical Analysis

Beijing ZHONGHUA SHENJING JINGSHENKE ZAZHI [CHINESE JOURNAL OF NEUROLOGY AND PSYCHIATRY] in Chinese No 1, 1981 pp 45-46

[Article by Lu Longguang [7627 7693 0342], Ma Wenhe [7456 2429 0735], Zhang Xinpao [1728 1800 0202], and Zhao Xiaoli [6392 2556 7787] of the Nanjing Psychiatric Hospital: "The Experience of Outpatient Electric Shock Treatment; Clinical Analysis of 800 Cases"]

[Text] Electric shock therapy already has a history of 40 years. Its active function in psychiatric treatment has been affirmed by the world's nations for a long time. To explore the clinical value of electric shock therapy before administering antipsychotic medication, we reviewed 1,542 cases of various types of psychosis which received outpatient electric shock therapy within the 3 years from 1952 to 1954. Of these, information on 800 cases was complete. The following is a report of the effectiveness of treatment and a review of some of the cases:

Analysis of Information

1. Sex and age: In this group, 412 cases were males, and 388 cases were females. Eight cases were less than 15 years old, 91 cases were between 16 and 20 years old, 389 cases were between 21 and 30 years old, 178 cases were between 31 and 40 years old, 93 cases were between 41 and 50 years old, 36 cases were between 51 and

60 years old, 2 cases were between 61 and 70 years old, and 1 case was over 70 years old. The ages of the patients receiving treatment were between 13 and 71 years old; 650 cases (81 percent) were between 21 and 50 years old. Those under 15 and over 50 totaled 49 cases.

2. Frequency of treatment: This group received a total of 6,543 electric shock treatments. Each person received an average of 6.1 treatments; the maximum number of treatments given to one patient was 38; the minimum number of treatments given to one patient was one.

3. Effectiveness of treatment:

(1) Type of disease and effectiveness of treatment within a short period: In the various types of psychosis, the best result was in the treatment of melancholia and mania, the percentages of cure in these diseases being 89.9 percent and 86.7 percent, respectively. The percentage of cure for affective psychosis was 82.2 percent. These were for the most part acute cases. While they were being administered electric shock therapy, most cases received psychotherapy. The percentage of cure for compulsive neurosis was 44.4 percent, while for schizophrenia it was 40.4 percent (Table 1).

Table 1. Type of Disease and Effectiveness of Treatment Within a Short Period

	(8)	(9)	(10)	(11)	(12)	(13)		
(1)	A	S	E	VIS	I	S	R	All
(2) Schizophrenia	105	29.0	108	29.1	192	36.5	21	23.0326
(3) Mania	60	79.0	6	7.5	6	7.5	4	6.375
(4) Depression	54	60.7	26	29.2	8	1.4	4	4.589
(5) Affective psychosis	54	69.3	21	23.1	12	33.3	4	4.491
(6) Compulsive neurosis	2	31.1	6	33.3	8	44.4	2	31.138
(7) Total	375	34.2	167	26.9	223	37.9	35	36.9300

Key:

1. Types
2. Schizophrenia
3. Mania
4. Depression
5. Affective psychosis
6. Compulsive neurosis
7. Total
8. Cured
9. Number of cases
10. Visible improvement
11. Improvement
12. Ineffective
13. Total

(2) Duration of disease and effectiveness of treatment within a short period: The percentage of patients cured within 1 year of the disease was 67.2 percent, the percentage of patients cured within 1 to 2 years was 59.9 percent, the percentage of patients cured within 2 to 3 years was 41.8 percent, the percentage of patients cured within 3 to 5 years was 34 percent, and the percentage of patients cured after 5 years of the disease was 32 percent. The shorter the history of the disease, the higher the effectiveness; this [finding] is consistent with domestic and foreign reports. The percentage of cure for patients with chronic disease of over 2 years' duration is still optimistic (Table 2).

Table 2. Duration of Disease and Effectiveness of Treatment Within a Short Period

	(1)	(2)	(4)	(5)	(6)	(7)			
Duration	N	%	N	%	N	%	Ave.		
< 1	178	44.8	63	22.1	63	22.1	43	10.8	397
1 ~	43	17.4	26	27.4	29	25.7	17	14.8	115
2 ~	27	24.1	19	17.3	33	30	31	28.2	110
3 ~	18	16	16	18	20	19	27	27	100
≥ 5	9	11.5	16	20.5	35	41.9	18	23.1	78

Key:

1. Duration of disease (year)
2. Cured
3. Number of cases
4. Visible improvement
5. Improvement
6. Ineffective
7. Total

4. Complications: Among the complications during the period of treatment of this group, failing memory was the most commonly seen, there being 28 cases or 3.5 percent. This complication occurred mostly after three to eight treatments. Headaches occurred in 25 cases (3.1 percent), all during the first few treatments. Spinal pain occurred in 23 cases (2.9 percent). Physical and X-ray examinations revealed one case (0.1 percent) of compressed fracture of the thoracic vertebrae. Bleeding of the gums occurred in 22 cases (2.8 percent). Injury of bitten tongue occurred in 14 cases (1.8 percent). Pain in the shoulder and knee joints occurred in 14 cases (1.8 percent). Mental disturbance occurred in 8 cases (1 percent) (including semiconsciousness, acute manic activity, and anxiety which were psychotic symptoms not seen in the original disease). Breathing difficulty occurred in 5 cases (0.6 percent), loosening of the front teeth occurred in 2 cases (0.3 percent), and aspiration pneumonia occurred in 1 case (0.1 percent).

The number of complications as reported was not uniform. The causes of the complications of this group included not only the effects of the treatment itself, but also a lack of technical skill, insufficient pretreatment preparation, and failure to follow normal procedures.

The question of deaths: Since our hospital's outpatient service began using electric shock therapy, several tens of thousands of treatments have been administered, and there has not been a single case of death. Thus it can be seen that this is still a relatively safe type of physical therapy.

5. Long-term effectiveness of electric shock therapy for schizophrenia: Of the 526 cases of schizophrenia, 190 cases reported results of followup visits according to the outpatient followup visit and observation records. In some of the cases, aftereffects of insomnia and such symptoms of neurosis remained after conditions improved. Except for a few patients of this group who regularly took sedatives and sleeping pills, no other treatment was given. Of the 53 cases of followup visits within 1 year, 67.4 percent remained cured or showed visible improvement. Of the 44 cases of followup visits 3 to 5 years after treatment, 47.7 percent remained cured or nearly cured (Table 3).

Table 3. Effectiveness of Followup Treatment of 190 Schizophrenic Cases

随访时间 (年)	(1)		(2)		(3)		(4)		(5)		(6)	
	数 (7)	% (%)	总计 数 (6)	% (%)								
<1	34	64.1	3	5.7	7	13.2	9	17.0	53			
1~	34	66.7	5	9.8	3	5.9	9	17.0	51			
2~	20	62.5	5	15.6	5	15.6	2	6.3	32			
3~	17	58.6	4	9.1	4	9.1	19	43.2	44			
>5	4	40.0	2	20.0	2	20.0	2	20.0	10			
(6)总计	109	57.4	19	10	21	11.1	41	21.5	190			

Key:

1. Time of followup visit (year)
2. Cured
3. Visible improvement
4. Improvement
5. Ineffective
6. Total
7. Number of cases

Discussion

Electric shock is a kind of physical therapy. Because the modus operandi of this kind of treatment is special, and because of the strong reaction of the patients, evaluation [of the treatment] has not been consistent since its inception. But because of its true effectiveness, it has thus been used continuously. This therapy was once banned from use during the latter part of the 1960's and the early 1970's in our nation. At present, most hospitals have revived its use, but the number of cases treated and the frequency of application have lessened. The same situation exists abroad. To explore the clinical value of electric shock therapy, we have summarized and reviewed past work and have proposed some views.

1. As the methods of treatment of psychosis continue to improve, the effectiveness of treatment has also gradually increased, especially during the past more than 20 years. The emergence and the rapid development of antipsychotic medicines have opened up a wide field for the treatment of psychosis, replacing most of the functions of electric shock therapy. Overall measurement of the information of this group shows that the method of electric shock is still an effective treatment for some types of psychosis, especially for melancholia and serious suicidal cases. Antipsychotic drugs can be used in coordination with it, but they cannot replace its function.

2. Of the 800 cases of psychotic patients subjected to electric shock therapy, 54.8 percent were cured by short-term treatment, and the effectiveness was 83 percent. The effectiveness of treatment of melancholia was 95.5 percent, the effectiveness of treatment of mania was 94.7 percent, and the effectiveness of treatment of schizophrenia was 76.9 percent. Outpatient cases followed up for between half a year and 5 years numbered 190; the percentage of those cured was 67.4 percent, and the effectiveness was 79 percent. This figure is definitely convincing. Foreign reports have pointed out that both before and after antimelancholia drugs came on the market, electric shock therapy has always been an outstandingly effective method for ameliorating melancholia, controlling suicidal tendencies, and consolidating the effectiveness of treatment. Facing the threat of serious suicidal tendencies, it can rapidly improve and eliminate the symptoms. Some people have dubbed it a "lifesaving treatment." Hoffet pointed out that the effectiveness of treatment of melancholia by promethazine is 54.5 percent, while the effectiveness of electric shock therapy is 95 percent. The effectiveness of treating schizophrenia with a touch of melancholia is 83.5 percent, which is a higher percentage than if only antipsychotic drugs are used. The complications of electric shock therapy are no greater than those in using antipsychotic drugs, and the death rate is the same. Negating electric shock therapy too early lacks sufficient factual basis.

We believe that continued use of electric shock therapy should require a strict selection of the cases, so as to grasp the suitable indications and contraindications. A detailed and careful physical examination should be carried out prior to treatment in order to profoundly grasp the overall situation of the advantages and the shortcomings. Patients with serious suicidal tendencies should be considered for electric shock therapy first if there are no contraindications. Refusal to eat, stiffness, psychomotor excitation with symptoms of aggressive attack on other people and self-mutilation which are difficult to control, and catatonic schizophrenia accompanied by a touch of melancholia are all suitable indications for this method of treatment. Information of this nature shows that patients who react well to electric shock therapy generally will respond well to treatment after two or three treatments. If there is still no improvement after more than five treatments, it will be difficult to obtain satisfactory results if treatment is continued. Also, some complications such as mental disturbance and memory disturbance all occur after eight treatments; this coincides with the reports in medical documents concerning the direct proportion between the seriousness of memory disturbance and the frequency of electric shock treatments. The patient being older than 50 years of age, relatively poor physical health, or psychosis accompanied by cardiovascular disease should be contraindications. Young people

under 15 years of age have not fully matured, and such treatment should be strictly limited. According to reports, analysis of the cause of death in electric shock therapy reveals that cardiovascular disease, prostrated breathing, and cerebro-vascular disease are the three most frequently seen causes. These can serve as references.

9296

CSO: 4008/375

END

**END OF
FICHE**

**DATE FILMED
6 Aug 1981**